EUROPEAN ORGANIZATION FOR NUCLEAR RESEARCH (CERN)

CERN-PH-EP/2011-092
2011/10/07

CMS-HIN-10-001

Dependence on pseudorapidity and on centrality of charged hadron production in PbPb collisions at $\sqrt{s_{\mathrm{NN}}} = 2.76$ TeV

The CMS Collaboration*

Abstract

A measurement is presented of the charged hadron multiplicity in hadronic PbPb collisions, as a function of pseudorapidity and centrality, at a collision energy of 2.76 TeV per nucleon pair. The data sample is collected using the CMS detector and a minimum-bias trigger, with the CMS solenoid off. The number of charged hadrons is measured both by counting the number of reconstructed particle hits and by forming hit doublets of pairs of layers in the pixel detector. The two methods give consistent results. The charged hadron multiplicity density, $dN_{\mathrm{ch}}/d\eta|_{\eta=0}$, for head-on collisions is found to be 1612 ± 55, where the uncertainty is dominated by systematic effects. Comparisons of these results to previous measurements and to various models are also presented.

Submitted to the Journal of High Energy Physics

*See Appendix A for the list of collaboration members

1 Introduction

Quantum chromodynamics (QCD), the theory of strong interactions, predicts a phase transition at high temperature between hadronic and deconfined matter [1]. Strongly interacting matter under extreme conditions can be studied experimentally using ultrarelativistic collisions of heavy nuclei. The field entered a new era in November 2010 when the Large Hadron Collider (LHC) produced the first PbPb collisions at a centre-of-mass energy per nucleon pair of 2.76 TeV. This represents an increase of more than one order of magnitude over the highest-energy nuclear collisions previously achieved in the laboratory. The multiplicity of charged particles produced in the central-rapidity region is a key observable characterising the properties of the quark-gluon matter created in these collisions [2].

Nuclei are extended objects, and their collisions occur at various impact parameters, referred to as "centralities". The studies of the dependence of the charged particle density on the type of colliding nuclei, on the centre-of-mass energy, and on the collision geometry are important for understanding the relative contributions of hard scattering and soft processes to particle production and provide insight into the partonic structure of the nuclei.

In this paper we report measurements of the multiplicity density $dN_{\mathrm{ch}}/d\eta$ of primary charged hadrons. The analysis is based on the 2.76 TeV-per-nucleon PbPb collision data recorded by the Compact Muon Solenoid (CMS) detector in December 2010, in runs without magnetic field. The pseudorapidity is defined as $\eta = -\ln[\tan(\theta/2)]$ with θ the polar angle with respect to the counterclockwise beam direction (the z axis). The number of primary charged hadrons N_{ch} is defined as all charged hadrons produced in an event including decay products of particles with proper lifetimes less than 1 cm.

A detailed description of the CMS experiment can be found in Ref. [3]. The pixel tracker used for the analysis covers the region $|\eta| < 2.5$ and a full 2π in azimuth, with 66M detector channels out of which 97.5% were functional during data taking. It consists of a three-layer barrel pixel detector (BPIX) and two endcap disks at each barrel end. Only the barrel section was used in this analysis. The first BPIX layer is located at a radius between 3.6 and 5.2 cm from the beam line, the second between 6.6 and 8.0 cm, and the third between 9.4 and 10.8 cm. The detectors used for event selection are the hadron forward (HF) calorimeters, which cover the region $2.9 < |\eta| < 5.2$, the beam scintillator counters (BSC), in the range $3.23 < |\eta| < 4.65$, and the beam pick-up timing (BPTX) devices located at $z = \pm 176$ m from the interaction point. The operation of the CMS detector with zero magnetic field has the benefit of an increase in the acceptance for charged hadrons down to $\sim$30 MeV/c transverse momentum (p_{T}) without the drawbacks from particles with small p_{T} curling up in the magnetic field. The nonzero p_{T} threshold is due to the 0.8 mm-thick beryllium beampipe, which is not penetrable for pions and protons below $p_{\mathrm{T}} \approx$30 and 140 MeV/c, respectively. The loss of particles due to the beampipe is estimated to be less than 1 percent of the produced primary charged hadrons.

Two analysis methods were used for the measurements of $dN_{\mathrm{ch}}/d\eta$ as a function of η and centrality: one uses only pixel clusters in single BPIX layers (hit-counting method), and the other uses doublets of pixel clusters reconstructed from pairs of BPIX layers (tracklet method).

The application of the pixel hit-counting method is a demonstration of the excellent pixel detector response and of its low occupancy even in this high-multiplicity environment, as well as the absence of noise and background. This method is not sensitive to detector misalignment or vertex-position resolution. The tracklet method is essentially a coincidence version of hit-counting. Using the angular coincidence of two hits from the same particle in different layers of the BPIX has the important feature of suppressing random noise.

The paper is organized as follows. The triggering and event selection requirements are explained in Section 2, followed by the description of the determination of the reaction centrality in Section 3. Sections 4 and 5 introduce the hit-counting and the tracklet methods, respectively. The systematic uncertainties are discussed in Section 6, while the final results are presented in Section 7.

2 Trigger and event selection

The expected cross section for PbPb hadronic inelastic collisions at $\sqrt{s_{NN}} = 2.76$ TeV is 7.65 b, according to the chosen Glauber MC parameters described in Section 3. Electromagnetic interactions of the colliding nuclei at large impact parameter (ultraperipheral collisions, UPC) can lead to the breakup of one or both Pb nuclei with a much higher cross section.

Minimum-bias (hadronic inelastic) collisions were selected by the Level-1 trigger system combining the logical OR of two clean and highly efficient triggers. One of them was the BSC coincidence, which requires at least one segment of the BSC firing on each side of the interaction point. The other was an HF coincidence trigger, which requires at least one HF tower on each side to have deposited energies that exceed the readout threshold. Both triggers accept noise at a low rate (less than 1 Hz with two noncolliding beams at full intensity), and have a very high efficiency (approximately 99% after the requirement of a reconstructed vertex). In order to suppress noncollision-related noise, cosmic-ray events, radioactivation, instrumental multiple triggering effects, and beam background, two colliding ion bunches were required to be present in coincidence with each one of these triggers, using information from the BPTX devices. The HF and BSC coincidence triggers were found to be largely insensitive to single-dissociation UPC, as discussed at the end of this section.

The collision rate was 1.0–1.85 Hz per colliding bunch pair during the PbPb data taking period. Therefore, with an orbit frequency of 11 245 Hz, the average number of collisions per bunch crossing was 0.9–1.6 $\times 10^{-4}$. There were 129 $\times$ 129 colliding bunches in the LHC at the time of data taking with no CMS magnetic field.

In order to reject beam-gas interactions, large-hit-multiplicity beam background, and UPC, several offline event selection requirements were imposed:

- Events containing beam-halo muons and other particles from upstream collisions were identified and excluded from the analysis, by requiring the time difference between two hits from the BSC stations on opposite sides of the interaction point to be within 20 ns of the mean flight time between them (73 ns).
- The large-multiplicity beam-background events were removed by requiring the compatibility of the observed pixel-cluster lengths (defined in Section 4) with the hypothesis of a PbPb interaction. This filter is the same as the one used in Ref. [4].
- An HF coincidence requirement was imposed. At least 3 HF towers were required on each side of the interaction point with at least 3 GeV total deposited energy in each tower.
- Furthermore, the presence of a reconstructed event vertex was required. The analysis methods use their corresponding analysis objects (pixel clusters and tracklets, respectively) to reconstruct the interaction point. The vertex reconstruction is only done along the beamline; the transverse position of the vertex is taken to be that of the beam axis [5]. The methods to determine the collision vertex are described in Sections 4.1 and 5.1.

The measurement of the $dN_{\mathrm{ch}}/d\eta$ distributions was performed using 100 031 events, corresponding to an integrated luminosity of 13 mb^{-1}. Correction factors were determined using simulated events generated with the AMPT Monte Carlo (MC) [6] program. This program combines the HIJING event generator [7] with the ZPC parton cascade procedure [8] and the ART relativistic transport model [9] for the last stage of parton hadronization. The default tune is used, and the simulated events are reconstructed with the same version of software as used to process the collision data. This event generator produces a larger tail in the multiplicity distribution than that observed in data, making the entire observed multiplicity region completely covered in the simulation. The charged hadron multiplicity in the most-central collisions is 20% higher in AMPT than in data, but since the analysis is done in bins of multiplicity, it is insensitive to this difference.

The event selection for hadronic collisions was fully efficient for (mid)central PbPb collisions. For peripheral collisions the event selection efficiency was determined by comparing peripheral PbPb data and $\sqrt{s} = 2.76$ TeV pp data with the AMPT and PYTHIA Z2 [10] simulations. Based on these studies, the total event selection efficiency of the minimum-bias trigger for events produced in hadronic PbPb interactions was found to be $(99 \pm 1)\%$.

The UPC contamination in the selected event sample was estimated using the photo-dissociation simulations from Ref. [11]. The single-lead photo-dissociation events were found to be 100% rejected by the event selection criteria outlined above, while half of the double-lead photo-dissociation events are found to pass the minimum-bias trigger. Such a UPC contamination amounts to $(1 \pm 0.5)\%$ of the total number of events collected and populates $\approx$15% (5%) of the 95–100% (90–95%) most peripheral (largest-centrality) events, being negligible for the remaining 0–90% fraction of the PbPb cross section.

3 Centrality determination

In studies with heavy ions, it is important to determine the degree of overlap of the two colliding nuclei, the so-called centrality of the interaction. Centrality is estimated using the sum of transverse energy in towers from both HF at positive and negative z positions. The distribution of the total transverse energy, after the trigger efficiency and the UPC corrections, was used to divide the event sample into bins, each representing 5% of the total nucleus-nucleus interaction cross section. The bin corresponding to the most central events (i.e. smallest impact parameter) is the 0–5% bin, the next one is 5–10% and so on. The distribution of the HF signal, along with the cuts used to define the various event classes, is shown in Fig. 1. The UPC are concentrated in the two most-peripheral bins. To avoid them completely, only the 0–90% bins are used for the measurements reported in this paper.

The centrality binning using equal fractions of the total interaction cross section can be correlated with more detailed properties of the collision. The quantity of interest for this measurement is the total number of nucleons in the two Pb nuclei that experienced at least one inelastic collision, N_{part}. The average values of N_{part} for the various centrality bins (from most-central to most-peripheral), together with their uncertainties, are given in Table 1. The N_{part} values were obtained using a Glauber MC simulation [12, 13] with the same parameters as in Ref. [14]. These calculations were translated into reconstructed centrality bins using correlation functions between N_{part} and the measured total transverse energy, obtained from AMPT simulated events. Different Glauber MC samples were produced varying the Glauber parameters within the uncertainties from Refs. [15] and [16]. The variation in the final results is quoted as the uncertainty in N_{part}.

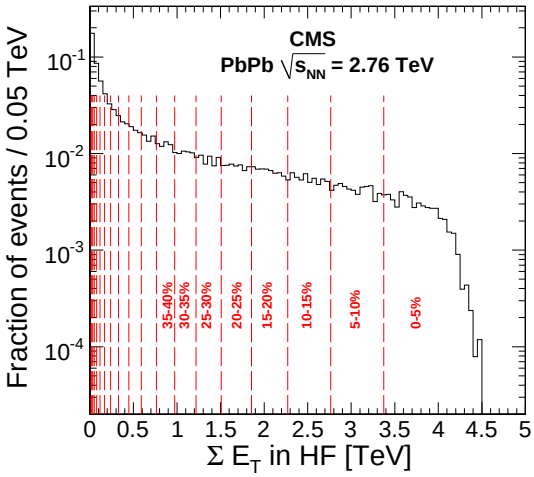

Figure 1: Distribution of the total transverse energy in the HF used to determine the centrality of the PbPb interactions. The centrality boundaries for each 5% centrality interval are shown by the dashed lines.

Table 1: Average N_{part} values and their uncertainties for each PbPb centrality range defined in 5 percentile segments of the total inelastic cross section. The values were obtained using a Glauber MC simulation with the same parameters as in Ref. [14].

Centrality	0–5%	5–10%	10–15%	15–20%	20–25%	25–30%
N_{part}	381 ± 2	329 ± 3	283 ± 3	240 ± 3	203 ± 3	171 ± 3
Centrality	30–35%	35–40%	40–45%	45–50%	50–55%	55–60%
N_{part}	142 ± 3	117 ± 3	95.8 ± 3.0	76.8 ± 2.7	60.4 ± 2.7	46.7 ± 2.3
Centrality	60–65%	65–70%	70–75%	75–80%	80–85%	85–90%
N_{part}	35.3 ± 2.0	25.8 ± 1.6	18.5 ± 1.2	12.8 ± 0.9	8.64 ± 0.56	5.71 ± 0.24

4 Hit-counting method and corrections

Charged particles traversing the pixel detector deposit a certain energy in the silicon sensors, resulting in a proportional amount of charge collected in the pixel readout cells. Contiguous pixel cells with charge above the readout threshold are merged into a pixel cluster. A pixel cluster might be split into multiple clusters if one of its pixel cells fluctuates below the threshold. This phenomenon is called cluster splitting. The fraction of split clusters was estimated from the cluster-to-cluster distance distribution. The fractions in data and simulation were found to differ by less than 0.6%. The pixel-cluster efficiency (i.e. the probability that a cluster is detected once a charged particle crosses a pixel-detector layer), as well as the fraction of large clusters split into two are important quantities for the measurement.

The pixel-cluster efficiency has been extensively studied in pp collisions [4, 17], indicating an efficiency of $(99.5 \pm 0.5)\%$. Despite larger particle multiplicities in PbPb collisions, the occupancy of the pixel detector is still smaller than 1% owing to its high granularity (whereas in the strip detector it reaches 20%), and the pixel detector exhibits the same excellent perfomance in PbPb as in pp collisions.

The hit-counting measurement method is based on the correlation between the cluster length in z and the pseudorapidity of a particle originating from the interaction point. It measures the primary charged hadron multiplicity distributions using the occupancy of a certain layer of the

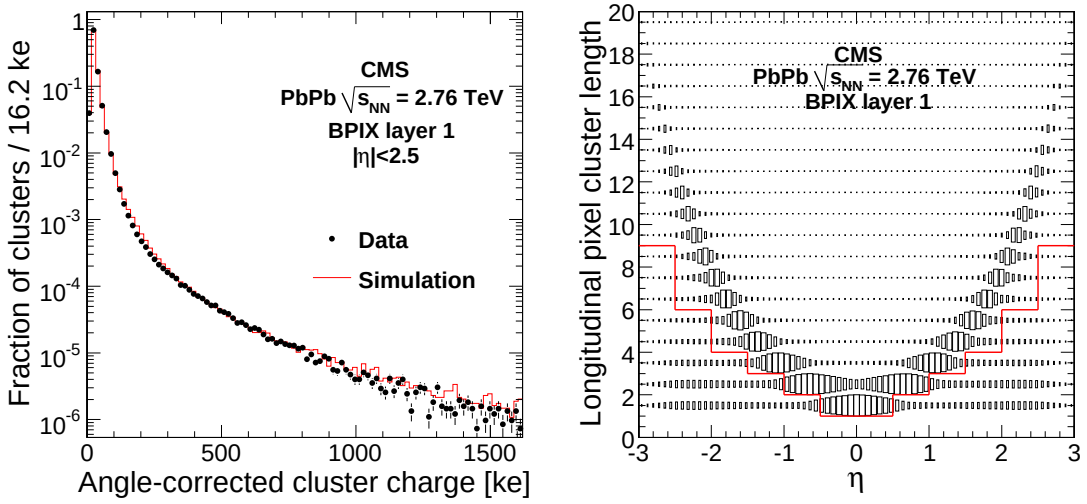

Figure 2: *Left*: Distribution of the angle-corrected pixel-cluster charge in units of equivalent kilo-electrons from 2.76 TeV PbPb data and simulation. *Right*: Pixel-cluster length along the beam direction in units of pixel cells for hits from the first layer of the BPIX, as a function of η after the event selection. The solid red line shows the selection on the minimum cluster length used in the analysis.

pixel detector by counting the reconstructed hits. The hit-counting method gives three largely independent measurements for the three barrel layers. A similar method was used by the PHOBOS experiment at RHIC [18] and also by CMS for earlier pp analyses [4, 17]. One of the disadvantages of the method is the strong reliance on detector simulation for correction factors. Therefore, the detector simulation was extensively studied and carefully compared to data. The simulation was found to give a very good description of the data in all observables related to detector performance. Such an example can be seen in the left panel of Fig. 2, which shows the distribution of the pixel-cluster charge in the first BPIX layer from data and simulation. Clusters were selected according to the cluster-size selection described in Section 4.2, and the cluster charge was normalised by the impact angle estimated from the cluster location and vertex position. The simulation describes the data well over six orders of magnitude.

4.1 Primary vertex reconstruction using clusters

There is a linear relationship between the length of a pixel-cluster along the beam direction and the z position of the cluster. Thus, hits from primary tracks leave a characteristic V-shaped pattern in the plane of cluster size versus z position. Nonprimary hits (e.g. due to secondary particles or nuclear interactions) fall mostly outside this V-shaped region. Thus, a V-shaped band is used to scan the z axis; the z position with the largest number of associated clusters is used as the vertex z position. The vertex z position is thus obtained by maximizing the consistency of the pixel-cluster lengths and global z positions with a primary vertex hypothesis.

4.2 Cluster selection

Particles travelling from the primary vertex at a small angle with respect to the beam axis produce larger clusters in the BPIX layers than those at large angles. The cluster size is proportional to $|\sinh\eta|$, where the pseudorapidity η of the cluster is computed with respect to the reconstructed vertex (right panel of Fig. 2). Particles from background processes (decays in flight, nuclear interactions, etc.) often have smaller clusters than those produced in the primary in-

teraction, since their crossing angle is not correlated to the η of the hit. Thus, a large fraction of clusters from background processes (refered to as background clusters) can be rejected by a selection based on the cluster size variable. The selection is defined in η bins (shown as a red line in the right panel of Fig. 2).

4.3 Corrections

Not all of the background clusters are removed by the cluster selection described above since they can occasionally mimic the length of clusters generated by primary particles. The correction factor $\chi(\eta, M)$ is defined as the ratio of the number of selected clusters in the data to the number of primary charged hadrons at a pseudorapidity η and a given cluster multiplicity M. It is calculated from simulation using:

$$\chi(\eta, M) = \frac{N_{\text{hit}}^{\text{MC}}(\eta, M)}{N_{\text{hadron}}^{\text{MC}}(\eta, M)}, \tag{1}$$

where M denotes the total number of clusters passing the cluster selection, $N_{\text{hit}}^{\text{MC}}(\eta, M)$ is the number of selected clusters, and $N_{\text{hadron}}^{\text{MC}}(\eta, M)$ the number of primary charged hadrons in the simulation. This correction factor is used to convert the measured $N_{\text{hit}}(\eta, M)$ pixel-cluster distributions from data into the corresponding primary charged hadron distributions, $N_{\text{hadron}}(\eta, M)$.

The $\chi(\eta, M)$ correction factor is only weakly dependent on the physical process producing the hadrons, since it mainly contains information on the detector geometry. In a perfectly hermetic and 100% efficient detector, $\chi(\eta, M)$ would be slightly above unity, as not only the primary, but also the secondary particles can generate hits. For detectors covering a limited solid angle, its values will be between 0 and 1. For very large multiplicities, $\chi(\eta, M)$ may decrease with increasing M because of the more significant occupancy (provided the primary/secondary ratio stays roughly constant). However, the occupancy of the silicon pixel layers is observed to be small and no apparent decrease of $\chi(\eta, M)$ is visible with increasing centrality. The χ correction increases with increasing distance from the interaction point, because layers further from the primary vertex are hit by more decay products, as well as by more secondaries from nuclear interactions.

The correction factor in the first layer is in the range 1.0–1.2, while its average value in the 0–10% centrality bin is 1.1, 1.2, and 1.3 for the first, second, and third layers, respectively.

The pseudorapidity distribution of charged particles, for a fixed M, is calculated from the measured $N_{\text{hit}}(\eta, M)$ distribution, correcting for the hit/primary charged hadron ratio and normalising it to the number of events with multiplicity M passing the event selection, $N_{\text{selected}}(M)$:

$$\frac{dN_{\text{ch}}}{d\eta}(\eta, M) = \frac{1}{\Delta\eta\, \chi(\eta, M)} \frac{N_{\text{hit}}(\eta, M)}{N_{\text{selected}}(M)}, \tag{2}$$

where $\Delta\eta$ is the width of the η bin.

The event selection efficiency for a given multiplicity is determined as the ratio of the number of MC events with multiplicity M which pass the event selection criteria $N_{\text{selected}}^{\text{MC}}(M)$ to the total number $N_{\text{tot}}^{\text{MC}}(M)$ generated with multiplicity M: $\epsilon(M) = N_{\text{selected}}^{\text{MC}}(M)/N_{\text{tot}}^{\text{MC}}(M)$.

To measure the final, multiplicity-independent pseudorapidity distribution, the multiplicity-dependent distributions derived from Eq. 2 are weighted by the event selection efficiency $\epsilon(M)$

and then summed over M:

$$\frac{dN_{\mathrm{ch}}}{d\eta}(\eta) = \frac{\sum_M N_{\mathrm{selected}}(M)\frac{1}{\epsilon(M)}\frac{dN_{\mathrm{ch}}}{d\eta}(\eta, M)}{\sum_M N_{\mathrm{selected}}(M)\frac{1}{\epsilon(M)}}. \tag{3}$$

Because a reconstructed event vertex is required as part of the event selection, the sum is over $M > 0$.

5 Tracklet method and corrections

Tracklets are two-hit combinations in different layers of the BPIX that are consistent with a particle originating from the primary vertex. The tracklet analysis makes use of the correlation between hit positions: pairs of hits produced by the same charged particle have only small differences in the pseudorapidity ($\Delta\eta$) and the azimuthal angle ($\Delta\phi$) with respect to the primary vertex.

5.1 Primary vertex reconstruction using tracklets

In this method a tracklet-based vertex finder is used. In the first step, a hit from the first BPIX layer is selected and a matching hit is sought. If the magnitude of the difference in azimuthal angle ($\Delta\phi$) between the two hits is smaller than 0.08, the pair is saved as a proto-tracklet. This procedure is repeated for each first-layer hit to get a collection of proto-tracklets. For each proto-tracklet, the expected longitudinal vertex position is found using:

$$z = z_1 - r_1(z_2 - z_1)/(r_2 - r_1), \tag{4}$$

where $z_{1(2)}$ is the z position of the first (second) layer hit, and $r_{1(2)}$ is its radius. The calculated z positions are saved as vertex candidates. The second step is to determine the primary vertex from the vertex candidates. If the magnitude of the difference between the z positions of any two vertex candidates is less than 0.14 cm, they are combined as a vertex candidate cluster. Finally, the vertex candidate cluster with the highest number of vertex candidates is selected as the primary vertex. The final vertex z position is determined by the average z position of the vertex candidates in the cluster.

5.2 Tracklet reconstruction

All three barrel layers of the pixel detector are used in pairs: 1st+2nd, 1st+3rd, and 2nd+3rd. The differences in pseudorapidity and azimuthal angle, as well as the two-dimensional separation $\Delta R = \sqrt{(\Delta\eta)^2 + (\Delta\phi)^2}$ between the two hits of a tracklet, are important for characterising the tracklet.

Tracklets are reconstructed in three steps:

1. For each reconstructed hit, the pseudorapidity is calculated using the primary vertex location. Hits that pass the cluster size selection (as described in Section 4.2) are kept for further analysis.

2. Starting with a reconstructed hit in the a^{th} layer and looping over the reconstructed hits in the b^{th} layer (with $b > a$), all possible combinations with $|\Delta R| < 0.5$ are saved as proto-tracklets.

3. Proto-tracklets are sorted in ΔR. If a b^{th}-layer hit is matched more than once, the proto-tracklet with the smallest ΔR is kept. The selected proto-tracklets are the final reconstructed tracklets.

In addition to primary charged particles, the set of tracklets also include contributions from secondary interactions in the beampipe, particles from weak decays, and combinatorial background.

The combinatorial background tracklets are defined as combinations from secondary hits and hits from different primary tracks. The background fraction is largely suppressed by the ΔR ordering and the selection of tracklets (described in the next section). The tracklets from secondary particles are suppressed, and the correction for the remaining contribution relies on simulation.

5.3 Combinatorial and secondary particle background

Background tracklets can be created from incorrectly associated hits. The $\Delta\eta$ and $\Delta\phi$ of a tracklet are very useful quantities for the separation of signal and combinatorial background tracklets. Because of the absence of magnetic field, selecting the best proto-tracklet with the smallest ΔR provides a powerful way to reject combinatorial background: signal proto-tracklets exhibit a correlation peak around $\Delta R = 0$, while the background component extends to large ΔR.

The $\Delta\eta$ and $\Delta\phi$ distributions of selected tracklets from minimum-bias collisions in data and simulation are shown in Fig. 3 for combinations in the first and second pixel layers. The signal peaks at $\Delta\eta$ and $\Delta\phi = 0$ are clearly visible. Data and simulation show agreement over several orders of magnitude.

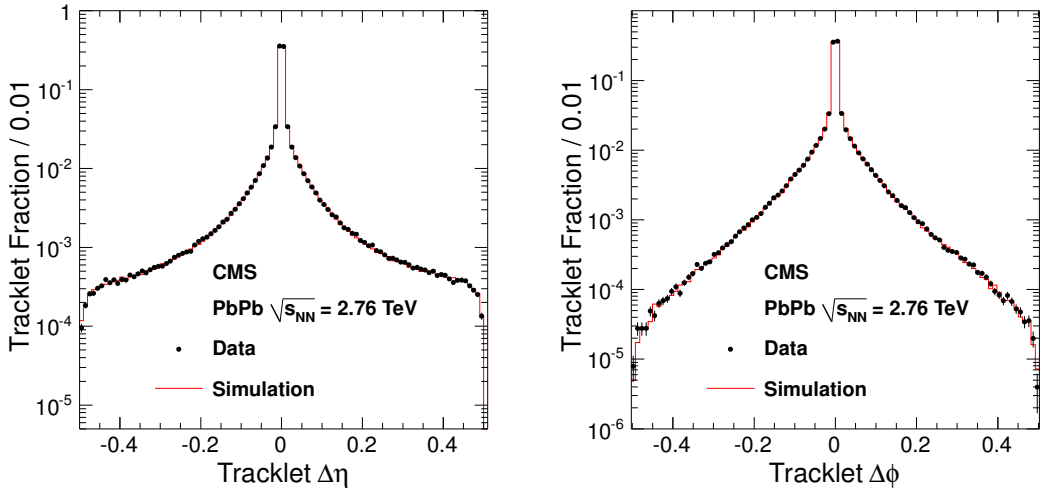

Figure 3: The (*left*) $\Delta\eta$ and (*right*) $\Delta\phi$ distributions for reconstructed tracklets in minimum-bias collisions from the first and the second pixel layers in data and simulation.

The effect of secondary hits on the agreement between data and simulation seen in Fig. 3 was tested by adding random hits to simulated events. The simulated tracklet spectra were found to be distorted even by a few percent of random hits, spoiling the agreement between data and simulation. Given the very good agreement in the tracklet spectra, the fraction β of combinatorial background tracklets can therefore be reliably obtained from simulation. The

value of β is in the range 0–15%, depending on the multiplicity of the event, the pseudorapidity of the tracklets, and the z position of the event vertex. The number of background-subtracted tracklets N_{tracklet} is determined from the raw number of tracklets in data $N^{\text{raw}}_{\text{tracklet}}$ using: $N_{\text{tracklet}} = (1-\beta) \times N^{\text{raw}}_{\text{tracklet}}$.

5.4 Efficiency and acceptance correction

To calculate the number of hadrons from the number of tracklets, an efficiency correction must be applied. The correction factor $\alpha(M, \eta, z_{\text{v}})$ for the tracklet reconstruction efficiency is defined as

$$\alpha(M, \eta, z_{\text{v}}) = \frac{N^{\text{truth}}_{\text{hadron}}(M, \eta, z_{\text{v}})}{[1-\beta(M, \eta, z_{\text{v}})] N^{\text{raw,MC}}_{\text{tracklet}}(M, \eta, z_{\text{v}})}, \tag{5}$$

where z_{v} is the z position of the vertex, $N^{\text{truth}}_{\text{hadron}}(M, \eta, z_{\text{v}})$ is the true number of charged hadrons in the simulated sample, and $N^{\text{raw,MC}}_{\text{tracklet}}$ is the raw number of selected tracklets in the MC sample. The factor $\alpha(M, \eta, z_{\text{v}})$ is used to calculate the charged hadron spectra from the measured background-subtracted tracklets. Typical values of α are less than 1.15 because of the high hit-reconstruction efficiency in the BPIX. At larger pseudorapidity, the correction factor increases, owning to the reduced acceptance. The size of the acceptance correction also depends on the position of the primary vertex.

The pseudorapidity distribution of charged hadrons for a given multiplicity M is obtained from the measured number of tracklets ($N^{\text{raw}}_{\text{tracklet}}$), the background fraction (β), the efficiency and acceptance correction (α), and the normalisation to the number of selected events:

$$\frac{dN_{\text{ch}}}{d\eta}(\eta, M) = \frac{\sum_{z_{\text{v}}} \alpha(M, \eta, z_{\text{v}})[1-\beta(M, \eta, z_{\text{v}})] N^{\text{raw}}_{\text{tracklet}}(M, \eta, z_{\text{v}})}{\Delta\eta \; N_{\text{selected}}(M)}, \tag{6}$$

where $\Delta\eta$ is the width of the η bin and $N_{\text{selected}}(M)$ is the number of selected events used in each multiplicity bin. The $\alpha(1-\beta)$ correction has a typical value larger than 0.85. For the final $dN_{\text{ch}}/d\eta$ distribution the multiplicity-dependent results are weighted by the event selection efficiency $\epsilon(M)$ and then summed as in Eq. 3.

6 Systematic uncertainties

A summary of systematic uncertainties affected the measurement of $dN_{\text{ch}}/d\eta$ for the two analysis methods is given in Table 2.

The results from different BPIX layers (or layer combinations) from either of the measurement methods differ by less than 2%, and thus they are averaged using the arithmetic mean. The uncertainties of the averaged results from the hit-counting and tracklet methods are dominately systematic and largely correlated. Therefore, the two results are averaged using equal weights. Since the difference between the measurements from the two methods is smaller than 1%, the weighting procedure has very little effect on the numerical value of the final result.

The uncertainties on the final average result are computed as follows. All the systematic uncertainties listed in Table 2 are correlated between the two methods, except those associated with the efficiency of reconstruction and misalignment. The correlated, $(s_{\text{h.c.}})_j$ and $(s_{\text{tracklet}})_j$, and

the uncorrelated, $(\sigma_{\text{h.c.}})_j$ and $(\sigma_{\text{tracklet}})_j$ uncertainties of the hit-counting and tracklet methods (indexed by j) are summed in quadrature:

$$\bar{s} = \sqrt{\Sigma_j[(s_{\text{h.c.}})_j + (s_{\text{tracklet}})_j]^2}/2 \text{ and } \bar{\sigma} = \sqrt{(\Sigma_j[(\sigma_{\text{h.c.}})_j^2 + (\sigma_{\text{tracklet}})_j^2]}/2, \quad (7)$$

resulting in $\bar{s}$ and $\bar{\sigma}$ correlated and uncorrelated uncertainties of the average, respectively. The total systematic uncertainty is then $\bar{\sigma}_{\text{tot}} = \sqrt{\bar{\sigma}^2 + \bar{s}^2}$.

In this paper the distributions of three observables are reported: $dN_{\text{ch}}/d\eta|_{\eta=0}$ as a function of centrality class, $(dN_{\text{ch}}/d\eta)/(N_{\text{part}}/2)$ as a function of η, and $(dN_{\text{ch}}/d\eta|_{\eta=0})/(N_{\text{part}}/2)$ as a function of N_{part}.

The systematic uncertainties affecting the slope and those affecting the absolute scale of $dN_{\text{ch}}/d\eta|_{\eta=0}$ and $(dN_{\text{ch}}/d\eta|_{\eta=0})/(N_{\text{part}}/2)$ measurements are determined separately. Systematic uncertainty sources affecting the slope are those on the centrality and the Glauber calculation of N_{part}; all other sources affect the scale. The results are presented in Section 7 with these two uncertainties shown separately.

The slope of $dN_{\text{ch}}/d\eta|_{\eta=0}$ as a function of centrality is only affected by the uncertainty on the determination of the centrality bins. Both the slope and the absolute scale of the N_{part}-normalised distributions are affected by the uncertainty on N_{part} from the Glauber calculation, given in Table 1. These contributions are computed by transforming the uncertainty in N_{part} into an uncertainty on the N_{part}-normalised hadron density distribution using the derivative of the measured $(dN_{\text{ch}}/d\eta)/(N_{\text{part}}/2)$ distributions as a function of N_{part}.

Table 2: Summary of systematic uncertainties on the $dN_{\text{ch}}/d\eta$ measurements and their sum for the two analysis methods.

Source	Hit-counting [%]	Tracklet [%]
Centrality (0–5% to 85–90%)	0.5–15.6	0.5–15.6
Pixel hit efficiency	0.5	1.0
Tracklet and cluster selection	3.0	0.5
Acceptance uncertainty	1.5	1.5
Correction for secondary particles	2.0	1.0
Pixel-cluster splitting	1.0	0.4
Reconstruction efficiency	-	1.9
Misalignment	-	1.0
Random hits	1.0	0.2
Total uncorrelated uncertainties	-	2.1
Total uncertainties	4.2–16.2	3.1–15.9

The systematic uncertainties affecting the measurements are as follows.

• **Centrality**: The determination of the centrality bins as a percentage of the total hadronic cross section relies on the hadronic event selection efficiency $(99 \pm 1)\%$, UPC contamination $(1 \pm 0.5)\%$, and the percentile binning of the centrality variable. Thus, the uncertainty in the event selection cross section causes uncertainty in the centrality binning by moving the bin boundaries, shifting the event population in each centrality bin. The effect of this centrality uncertainty on the final results was studied by repeating the analysis using various centrality tables (derived from the various trigger efficiencies allowed by the uncertainty on the efficiency). These studies indicate that the uncertainty of the $dN_{\text{ch}}/d\eta$ values ranges from 0.5% for the 0–5% centrality bin to 15.6% for the 85–90% centrality bin.

• **Pixel hit efficiency**: The efficiency of the pixel layers is larger than 99%, measured from pp data [17]. The pixel detector has low occupancy even in central heavy-ion collisions because of its fine segmentation. Therefore, the same pixel hit efficiency and uncertainty measured in pp collisions are used here. The pixel hit efficiency affects tracklets more, since two layers are required; a 0.5% inefficiency per pixel layer leads to a 1% inefficiency for tracklet finding.

• **Tracklet and cluster selection**: Varying the cluster selection requirements (pixel-cluster length selection) and tracklets selection (requirement on ΔR) is used to estimate the uncertainty due to cluster and tracklet selection. The cluster selections were changed by one pixel unit in all η bins and the ΔR selection by a factor of three. The observed differences in the final results (3% and 0.5%, respectively) are quoted as conservative systematic uncertainties.

• **Acceptance uncertainty**: The positions of the BPIX modules are only slightly different in data and in simulation, but hits at the extreme edges of the BPIX are not used in the analysis, limiting the systematic uncertainty from this effect. The η, ϕ acceptance was estimated from data by using the endpoints of tracklets to map the active surface of the BPIX layers. From this study, the acceptance correction is estimated to be 1% in pp collisions. In PbPb collisions (due to the longer luminous region in the beam direction) this uncertainty was increased to 1.5%. No correction is applied, but the effect is included in the systematic uncertainty.

• **Corrections due to hits from secondary particles**: The sensitivity of the correction factors applied to remove hits caused by secondary particles was tested using two largely different event generators: AMPT and HYDJET [19]. The relative fraction of strange particle production differs by 60% in the two generators, but the effect on the correction factor was found to be only 2% for the case of the hit-counting analysis. The tracklet analysis is less sensitive to secondaries.

• **Pixel cluster splitting**: The relative fraction of split clusters was estimated from the cluster-cluster distance distribution. This study shows that the number of split clusters in data does not exceed that in simulation by more than 0.5–0.7%. No correction is applied for this effect in the analyses, but a conservative systematic uncertainty (1% and 0.4%, respectively, for the hit-counting and tracklet analyses) is assigned.

• **Efficiency of tracklet reconstruction**: The uncertainties in the simulation of the p_{T} and multiplicity (M) distributions influence the determination of the tracklet reconstruction efficiency. The uncertainty (1.9%) is estimated based on variations of these quantities within reasonable limits: $\langle p_{\mathrm{T}} \rangle$ was modified by 10%, and the multiplicity variable was changed from using clusters to HF towers.

• **Misalignment**: The hit-counting method is not sensitive to detector misalignments. The tracklet method has a sensitivity through the ΔR selection, which was studied by moving the reconstructed hit positions (the entire detector) by 0.3 mm in the simulation, while keeping the vertex position at the same place, giving a 1% change in the final result. Since the $\Delta\phi$ and $\Delta\eta$ distributions and the correlation widths agree well, no significant misalignment is seen in the data.

• **Random hits**: With the restrictive event selection criteria, the contamination from beam-gas (high-occupancy) events in the final data sample is negligible. The other potential source of background is the accidental overlap between beam-gas and PbPb collisions. A conservative systematic uncertainty of 1% is assigned for the hit-counting analysis, which is more sensitive to this overlap than the tracklet analysis, for which 0.2% is assigned.

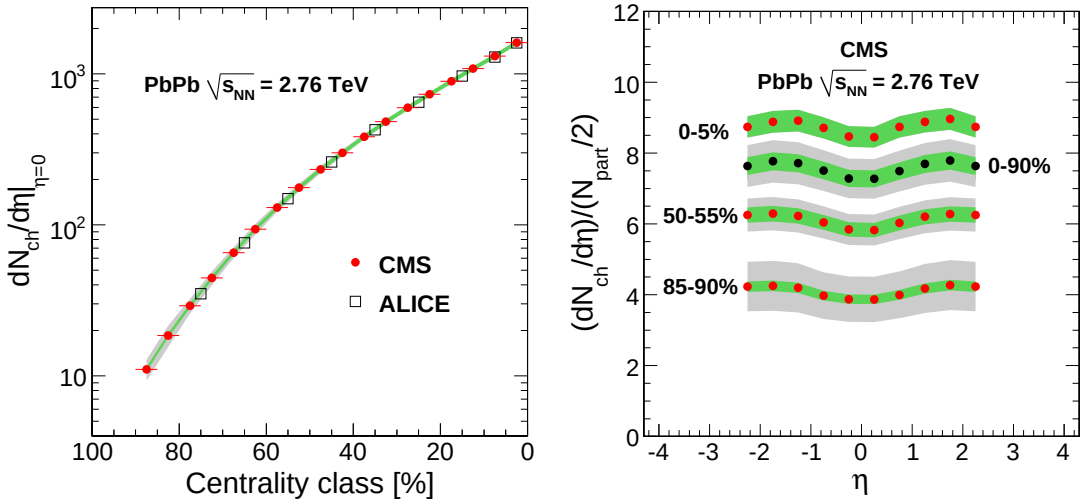

Figure 4: *Left*: $dN_{\mathrm{ch}}/d\eta|_{\eta=0}$ as a function of centrality class in 2.76 TeV PbPb collisions from this experiment (solid circles) and from ALICE (open squares) [20]. The inner green band shows the measurement uncertainties affecting the scale of the measured distribution from this analysis, while the outer grey band shows the full systematic uncertainty, i.e. affecting both the scale and the slope. *Right*: Measured $dN_{\mathrm{ch}}/d\eta/(N_{\mathrm{part}}/2)$ distributions from this analysis as a function of η in various centrality bins.

7 Results

The hit-counting and tracklet $dN_{\mathrm{ch}}/d\eta$ results are in good agreement; their average difference is smaller than 1%. Their individual results are averaged as described in Section 6, and these averages are presented as the final results.

The left panel of Fig. 4 presents the measured $dN_{\mathrm{ch}}/d\eta|_{\eta=0}$ values as a function of centrality. The statistical uncertainties are negligible, while the systematic uncertainties are shown as two bands. The inner green band shows the measurement uncertainties affecting the scale of the measured distribution, while the outer grey band shows the full systematic uncertainty, i.e. affecting both the scale and the slope. Details on the calculation of the uncertainty bands are given in Section 6. The charged hadron density for the 5% most-central events (0–5% centrality bin) is measured to be $dN_{\mathrm{ch}}/d\eta|_{\eta=0} = 1612 \pm 55\,(syst.)$. These results are consistent with those of ALICE [20] within the uncertainties, as shown in Fig. 4 (left). The error bars of the ALICE points in the figure show the total statistical and systematic uncertainties. The CMS measurements cover the centrality range of 0–90%, extending the ALICE results (0–80%) to more-peripheral collisions.

In order to compare bulk particle production for different colliding nuclei and at different energies, the charged-hadron density is divided by the average number of participating nucleon pairs, $N_{\mathrm{part}}/2$, determined for each centrality bin. The N_{part} values are obtained using the Glauber calculation, by classifying events according to their impact parameter, without reference to a specific particle production model (Table 1).

The measured $(dN_{\mathrm{ch}}/d\eta)/(N_{\mathrm{part}}/2)$ distributions as a function of η in various centrality bins are shown in the right panel of Fig. 4. The uncertainty bands of these distributions also include the Glauber uncertainty on N_{part}. The η dependence of the results is weak, varying by less than 10% over the η range. The slight dip at $\eta = 0$ is a trivial kinematic effect (Jacobian) owing to the use of pseudorapidity (η) rather than rapidity (y).

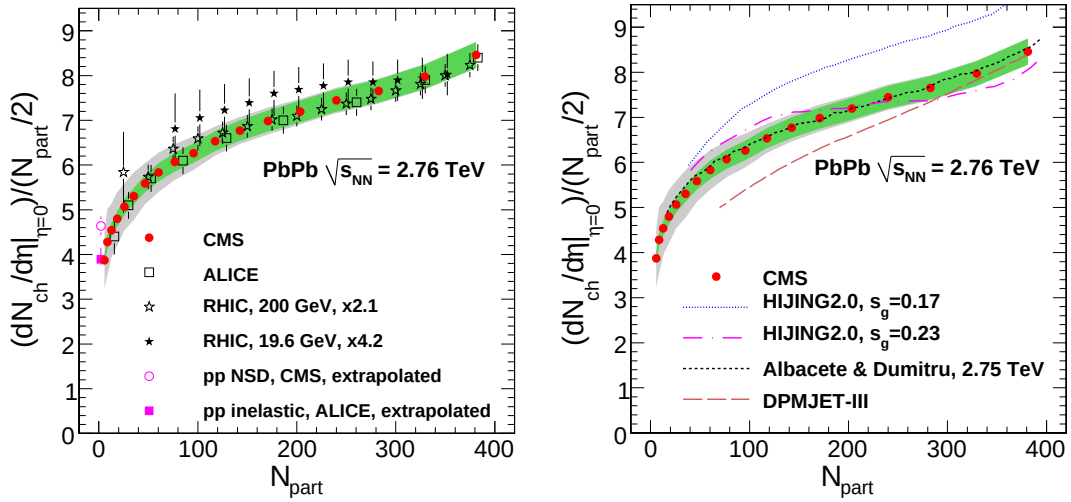

Figure 5: *Left*: Measured $(dN_{\rm ch}/d\eta|_{\eta=0})/(N_{\rm part}/2)$ as a function of the number of participants in 2.76 TeV PbPb collisions from this analysis and the ALICE experiment [20], from RHIC [21] at 200 GeV and 19.6 GeV, and from extrapolated pp results from CMS [17] and ALICE [22]. Systematic uncertainties affecting the scale of the measurements from this analysis are shown as inner green error bands and the total systematic uncertainties as an outer grey band, while the error bars indicate statistical uncertainties. The black stars are shifted slightly to the right for better visibility. The ALICE and the averaged RHIC results are from [20] and [21], respectively. *Right*: Results from this analysis are compared with model predictions of $(dN_{\rm ch}/d\eta|_{\eta=0})/(N_{\rm part}/2)$ as a function of the number of participants in 2.76 TeV PbPb collisions. The model predictions are taken from Refs. [23], [24], and [25].

The left panel of Fig. 5 presents the measured $(dN_{\rm ch}/d\eta|_{\eta=0})/(N_{\rm part}/2)$ as a function of $N_{\rm part}$. The statistical uncertainties on the CMS results are indicated by error bars (negligible), while the systematic uncertainties are shown as two bands. The inner green band shows the systematic uncertainty affecting the scale, while the outer grey band shows the full systematic uncertainty. The error bars on the ALICE [20] and the RHIC [21] points show the quadratic sum of the statistical and systematic uncertainties. The RHIC results are multiplied by numerical factors to match the $N_{\rm part}$-normalised multiplicity observed at the LHC for central collisions. The pp results shown in the figure are obtained from the measured non-single-diffractive (NSD) $dN_{\rm ch}/d\eta|_{\eta=0} = 4.47 \pm 0.2$ (CMS) [17] and the inelastic $dN_{\rm ch}/d\eta|_{\eta=0} = 3.77^{+0.26}_{-0.13}$ (ALICE) [22] values at 2.36 TeV, using the $\sqrt{s}$ dependence of the charged hadron multiplicity density measured in NSD and inelastic collisions from Ref. [4]. The error bars on the pp points show the total (statistical and systematic) uncertainties. The $N_{\rm part}$ values used for the normalisation by CMS and ALICE differ by less than 2%. Within the uncertainties, the $N_{\rm part}$-normalised hadron densities follow a similar dependence on centrality for all centre-of-mass energies, although the lower-energy collider data appear to have a flatter dependence on $N_{\rm part}$.

The phenomenological descriptions of particle production in nuclear collisions are often based on two-component models, combining contributions from perturbative QCD processes, i.e. (mini)jet fragmentation and soft interactions. The data are compared to three different approaches: (i) HIJING 2.0 [23], which basically scales (via the number of incoherent nucleon-nucleon collisions) the (semi)hard parton scatterings and fragmentation (Lund model [26]) implemented in PYTHIA after accounting for the "shadowing" of the nuclear parton distribution functions; (ii) parton saturation approaches [24], which model heavy-ion interactions as the

collision of two dense multigluon wavefunctions with cross sections peaking at a semihard scale (saturation momentum of ≈2–3 GeV/c at the LHC) [27, 28], followed by their fragmentation according to a simple parton-to-hadron local-duality prescription; and (iii) the DPMJET-III MC program [25], based on the Regge-Gribov theory. This is an extension of the PHOJET [29] program in which interactions from soft degrees of freedom (Pomerons) can fuse in the dense initial state. They are extended consistently into the hard regime via "hard" or "cut" Pomerons, and then fragmented using the standard Lund model.

The measured $(dN_{\mathrm{ch}}/d\eta|_{\eta=0})/(N_{\mathrm{part}}/2)$ versus N_{part} distribution is compared to the various model predictions in the right panel of Fig. 5. The two-component HIJING 2.0 model, which has been tuned to high-energy pp and central PbPb data, describes the general shape of the data. The HIJING model includes an impact-parameter-dependent gluon shadowing parameter s_g, which limits the rise of particle production with centrality. The magnitude of the particle production favours a relatively large $s_g = 0.23$ value, although the shape of the centrality dependence prefers a smaller $s_g = 0.17$. The observed centrality dependence is well reproduced by the saturation model of Ref. [24]. Both Refs. [23] and [24] were published knowing the result of ALICE [30] on the multiplicity of the 5% most-central collisions, although previous saturation-based calculations (e.g. [31]) predicted central charged hadron densities very similar to those finally measured. The DPMJET-III model is capable of describing the charged hadron multiplicity in the most-central collisions, but shows a stronger rise with centrality than observed in the data. The measured particle densities provide basic constraints on the initial conditions of the quark-gluon plasma in any hydrodynamical approach employed to study PbPb interactions at the LHC [32].

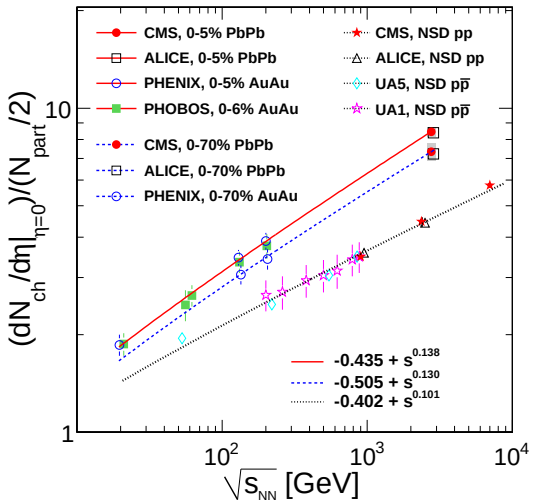

Figure 6: Normalized charged hadron pseudorapidity density at $\eta = 0$ as a function of centre-of-mass energy for the 0–5% most-central nucleus-nucleus collisions (top set of points) and 0–70% centrality (middle set), and for NSD pp collisions (bottom set). The fits to power-law functions are shown by lines. The grey band around the PbPb CMS points indicates the total systematic uncertainty. The statistical uncertainty is negligible. The error bars on the other points indicate statistical and systematic errors. The ALICE, PHENIX, and PHOBOS results (which are shifted slightly to the right for better visibility) are taken from Refs. [20], [21], and [33], respectively. The NSD pp results of CMS, ALICE, UA5, and UA1 are from Refs. [4, 17], [22], [34], and [35], respectively.

The collision-energy dependence of the measured $(dN_{\mathrm{ch}}/d\eta|_{\eta=0})/(N_{\mathrm{part}}/2)$ for 0–5% and 0–

70% centrality from this analysis and from ALICE, PHENIX, and PHOBOS can be seen in Fig. 6. The PHENIX and PHOBOS points are taken from Refs. [21] and [33], their error bars representing both the statistical and systematic uncertainties. Systematic uncertainties of the measurements from this analysis are shown as an error band, while the statistical uncertainties are negligible. The NSD pp results of CMS, ALICE, UA5, and UA1 are from Refs. [4, 17], [22], [34], and [35], respectively. The N_{part} values at different collision energies are different for a fixed centrality bin. When the N_{part} dependence of $(dN_{\mathrm{ch}}/d\eta)/(N_{\mathrm{part}}/2)$ from PHENIX and PHOBOS are used to extrapolate their $(dN_{\mathrm{ch}}/d\eta)/(N_{\mathrm{part}}/2)$ results shown in Fig. 6 to the N_{part} values appropriate for the LHC, they change by no more than 3%. This correction is not applied in Fig. 6. The normalised charged hadron densities shown in Fig. 6 are fit to a power-law function: $a + s_{\mathrm{NN}}^{n}$. The fit returns the value $n = 0.13$ for PbPb and $n = 0.10$ for NSD pp collisions. The results of the fits are shown by the straight lines in Fig. 6. These results provide additional constraints on the energy evolution of the saturation momentum in the proton and nuclei [27, 28], as well as in general on the p_{T} cutoff between soft and hard dynamics used in the models of particle production in high-energy hadronic collisions.

8 Summary

A measurement of charged hadron multiplicity as a function of pseudorapidity and centrality in PbPb collisions at $\sqrt{s_{\mathrm{NN}}} = 2.76$ TeV has been reported. For the 5% most-central collisions, a primary charged hadron density of 1612 ± 55 is measured, which represents an increase of a factor of 3 compared to similar measurements at RHIC energies. The $dN_{\mathrm{ch}}/d\eta$ distributions, measured over the range $|\eta| < 2.5$, show weak η dependence, the variation being less than 10%. The N_{part}-normalised multiplicity distributions from RHIC and the LHC have a similar dependence on centrality, although the lower-energy collider data has a somewhat flatter dependence. A parton saturation model describes well the observed centrality dependence. The collision-energy dependence of the measured hadron multiplicities at central rapidities is well modelled by a power-law function of the type $a + s_{\mathrm{NN}}^{n}$. These results provide information on the parton structure of the nucleus and the proton and its evolution as a function of centre-of-mass energy. They also give additional constraints on the initial conditions in nucleus-nucleus collisions at LHC energies for hydrodynamical evolution studies of the strongly interacting produced system.

Acknowledgments

We wish to congratulate our colleagues in the CERN accelerator departments for the excellent performance of the LHC machine. We thank the technical and administrative staff at CERN and other CMS institutes, and acknowledge support from: FMSR (Austria); FNRS and FWO (Belgium); CNPq, CAPES, FAPERJ, and FAPESP (Brazil); MES (Bulgaria); CERN; CAS, MoST, and NSFC (China); COLCIENCIAS (Colombia); MSES (Croatia); RPF (Cyprus); Academy of Sciences and NICPB (Estonia); Academy of Finland, ME, and HIP (Finland); CEA and CNRS/IN2P3 (France); BMBF, DFG, and HGF (Germany); GSRT (Greece); OTKA and NKTH (Hungary); DAE and DST (India); IPM (Iran); SFI (Ireland); INFN (Italy); NRF and WCU (Korea); LAS (Lithuania); CINVESTAV, CONACYT, SEP, and UASLP-FAI (Mexico); PAEC (Pakistan); SCSR (Poland); FCT (Portugal); JINR (Armenia, Belarus, Georgia, Ukraine, Uzbekistan); MST and MAE (Russia); MSTD (Serbia); MICINN and CPAN (Spain); Swiss Funding Agencies (Switzerland); NSC (Taipei); TUBITAK and TAEK (Turkey); STFC (United Kingdom); DOE and NSF (USA).

Individuals have received support from the Marie-Curie programme and the European Research Council (European Union); the Leventis Foundation; the A. P. Sloan Foundation; the Alexander von Humboldt Foundation; the Associazione per lo Sviluppo Scientifico e Tecnologico del Piemonte (Italy); the Belgian Federal Science Policy Office; the Fonds pour la Formation à la Recherche dans l'Industrie et dans l'Agriculture (FRIA-Belgium); and the Agentschap voor Innovatie door Wetenschap en Technologie (IWT-Belgium).

References

[1] F. Karsch and E. Laermann, "Thermodynamics and in-medium hadron properties from lattice QCD", (2003). arXiv:hep-lat/0305025.

[2] D. Kharzeev and M. Nardi, "Hadron production in nuclear collisions at RHIC and high density QCD", *Phys. Lett. B* **507** (2001) 121. doi:10.1016/S0370-2693(01)00457-9.

[3] CMS Collaboration, "The CMS experiment at the CERN LHC", *JINST* **03** (2008) S08004. doi:10.1088/1748-0221/3/08/S08004.

[4] CMS Collaboration, "Transverse-momentum and pseudorapidity distributions of charged hadrons in pp collisions at $\sqrt{s} = 7$ TeV", *Phys. Rev. Lett.* **105** (2010) 022002. doi:10.1103/PhysRevLett.105.022002.

[5] CMS Collaboration, "Tracking and Primary Vertex Results in First 7 TeV Collisions", *CMS Physics Analysis Summary* **CMS-PAS-TRK-10-005** (2010).

[6] Z.-W. Lin et al., "A multi-phase transport model for relativistic heavy ion collisions", *Phys. Rev. C* **72** (2005) 064901. doi:10.1103/PhysRevC.72.064901.

[7] X.-N. Wang and M. Gyulassy, "HIJING: A Monte Carlo model for multiple jet production in pp, pA, and AA collisions", *Phys. Rev. D* **44** (1991) 3501. doi:10.1103/PhysRevD.44.3501.

[8] B. Zhang, "ZPC 1.0.1: a parton cascade for ultrarelativistic heavy ion collisions", *Comput. Phys. Commun.* **109** (1998) 193. doi:doi:10.1016/S0010-4655(98)00010-1.

[9] B.-A. Li and C. M. Ko, "Formation of superdense hadronic matter in high energy heavy-ion collisions", *Phys. Rev. C* **52** (1995) 2037. doi:10.1103/PhysRevC.52.2037.

[10] T. Sjöstrand, S. Mrenna, and P. Skands, "PYTHIA 6.4 Physics and Manual", *JHEP* **05** (2006) 026. Tune Z2. doi:10.1088/1126-6708/2006/05/026.

[11] O. Djuvsland and J. Nystrand, "Single and Double Photonuclear Excitations in Pb+Pb Collisions at $\sqrt{s_{NN}} = 2.76$ TeV at the CERN Large Hadron Collider", (2010). arXiv:1011.4908v2.

[12] M. L. Miller et al., "Glauber modeling in high energy nuclear collisions", *Ann. Rev. Nucl. Part. Sci.* **57** (2007) 205. doi:10.1146/annurev.nucl.57.090506.123020.

[13] B. Alver et al., "The PHOBOS Glauber Monte Carlo", (2008). arXiv:0805.4411v1.

[14] CMS Collaboration, "Observation and studies of jet quenching in PbPb collisions at $\sqrt{s_{NN}} = 2.76$ TeV", (2011). arXiv:1102.1957v2. Submitted to Physical Review C.

[15] H. De Vries, C. W. De Jager, and C. De Vries, "Nuclear charge and magnetization density distribution parameters from elastic electron scattering", *Atom. Data Nucl. Data Tabl.* **36** (1987) 495. doi:10.1016/0092-640X(87)90013-1.

[16] B. Alver et al., "Importance of correlations and fluctuations on the initial source eccentricity in high-energy nucleus-nucleus collisions", *Phys. Rev. C* **77** (2008) 014906. doi:10.1103/PhysRevC.77.014906.

[17] CMS Collaboration, "Transverse-momentum and pseudorapidity distributions of charged hadrons in pp collisions at $\sqrt{s} = 0.9$ and 2.36 TeV", *JHEP* **02** (2010) 041. doi:10.1007/JHEP02(2010)041.

[18] PHOBOS Collaboration, "Charged-particle pseudorapidity density distributions from Au+Au collisions at $\sqrt{s_{NN}}$ = 130 GeV", *Phys. Rev. Lett.* **87** (2001) 102303. doi:10.1103/PhysRevLett.87.102303.

[19] I. P. Lokhtin and A. M. Snigirev, "A model of jet quenching in ultrarelativistic heavy ion collisions and high-p_{T} hadron spectra at RHIC", *Eur. Phys. J. C* **45** (2006) 211. doi:10.1140/epjc/s2005-02426-3.

[20] ALICE Collaboration, "Centrality dependence of the charged-particle multiplicity density at mid-rapidity in Pb-Pb collisions at $\sqrt{s_{NN}} = 2.76$ TeV", *Phys. Rev. Lett.* **106** (2011) 032301. doi:10.1103/PhysRevLett.106.032301.

[21] PHENIX Collaboration, "Systematic Studies of the Centrality and $\sqrt{s_{NN}}$ Dependence of the $dE_T/d\eta$ and $dN_{ch}/d\eta$ in Heavy Ion Collisions at Mid-rapidity", *Phys. Rev. C* **71** (2005) 034908. doi:10.1103/PhysRevC.71.034908.

[22] ALICE Collaboration, "Charged-particle multiplicity measurement in proton-proton collisions at $\sqrt{s} = 0.9$ and 2.36 TeV with ALICE at LHC", *Eur. Phys. J. C* **68** (2010) 89. doi:10.1140/epjc/s10052-010-1339-x.

[23] W.-T. Deng, X.-N. Wang, and R. Xu, "Gluon shadowing and hadron production in heavy-ion collisions at LHC", (2010). arXiv:1011.5907v1.

[24] J. L. Albacete and A. Dumitru, "A model for gluon production in heavy-ion collisions at the LHC with rcBK unintegrated gluon densities", (2010). arXiv:1011.5161v1.

[25] F. Bopp et al., "Inclusive distributions at the LHC as predicted from the DPMJET-III model with chain fusion", (2007). arXiv:0706.3875v1. Interpolated between 2.0 and 5.5 TeV values.

[26] B. Andersson et al., "Parton fragmentation and string dynamics", *Phys. Rept.* **97** (1983) 31. doi:10.1016/0370-1573(83)90080-7.

[27] F. Gelis, E. Iancu, J. Jalilian-Marian et al., "The Color Glass Condensate", *Ann. Rev. Nucl. Part. Sci.* **60** (2010) 463. doi:10.1146/annurev.nucl.010909.083629.

[28] D. Kharzeev, E. Levin, and L. McLerran, "Parton saturation and N_{part} scaling of semi-hard processes in QCD", *Phys. Lett. B* **561** (2003) 93. doi:10.1016/S0370-2693(03)00420-9.

[29] R. Engel, J. Ranft, and S. Roesler, "Hard diffraction in hadron-hadron interactions and in photoproduction", *Phys. Rev. D* **52** (1995) 1459. doi:10.1103/PhysRevD.52.1459.

[30] ALICE Collaboration, "Charged-particle multiplicity density at mid-rapidity in central Pb-Pb collisions at $\sqrt{s_{NN}}$ = 2.76 TeV", *Phys. Rev. Lett.* **105** (2010) 252301. doi:10.1103/PhysRevLett.105.252301.

[31] N. Armesto, C. A. Salgado, and U. A. Wiedemann, "Relating high-energy lepton hadron, proton nucleus and nucleus nucleus collisions through geometric scaling", *Phys. Rev. Lett.* **94** (2005) 022002. doi:10.1103/PhysRevLett.94.022002.

[32] T. Hirano, "Relativistic hydrodynamics at RHIC and LHC", *Prog. Theor. Phys. Suppl.* **168** (2007) 347. doi:10.1143/PTPS.168.347.

[33] B. Alver et al., "Charged-particle multiplicity and pseudorapidity distributions measured with the PHOBOS detector in Au+Au, Cu+Cu, d+Au, and p+p collisions at ultrarelativistic energies", *Phys. Rev. C* **83** (2011) 024913. doi:10.1103/PhysRevC.83.024913.

[34] UA5 Collaboration, "Scaling of Pseudorapidity Distributions at c.m. Energies Up to 0.9 TeV", *Z. Phys. C* **33** (1986) 1. doi:10.1007/BF01410446.

[35] UA1 Collaboration, "A study of the general characteristics of proton-antiproton collisions at $\sqrt{s} = 0.2$ to 0.9 TeV", *Nucl. Phys. B* **335** (1990) 261. doi:10.1016/0550-3213(90)90493-W.

A The CMS Collaboration

Yerevan Physics Institute, Yerevan, Armenia
S. Chatrchyan, V. Khachatryan, A.M. Sirunyan, A. Tumasyan

Institut für Hochenergiephysik der OeAW, Wien, Austria
W. Adam, T. Bergauer, M. Dragicevic, J. Erö, C. Fabjan, M. Friedl, R. Frühwirth, V.M. Ghete, J. Hammer[1], S. Hänsel, M. Hoch, N. Hörmann, J. Hrubec, M. Jeitler, W. Kiesenhofer, M. Krammer, D. Liko, I. Mikulec, M. Pernicka, B. Rahbaran, H. Rohringer, R. Schöfbeck, J. Strauss, A. Taurok, F. Teischinger, C. Trauner, P. Wagner, W. Waltenberger, G. Walzel, E. Widl, C.-E. Wulz

National Centre for Particle and High Energy Physics, Minsk, Belarus
V. Mossolov, N. Shumeiko, J. Suarez Gonzalez

Universiteit Antwerpen, Antwerpen, Belgium
S. Bansal, L. Benucci, E.A. De Wolf, X. Janssen, S. Luyckx, T. Maes, L. Mucibello, S. Ochesanu, B. Roland, R. Rougny, M. Selvaggi, H. Van Haevermaet, P. Van Mechelen, N. Van Remortel

Vrije Universiteit Brussel, Brussel, Belgium
F. Blekman, S. Blyweert, J. D'Hondt, R. Gonzalez Suarez, A. Kalogeropoulos, M. Maes, A. Olbrechts, W. Van Doninck, P. Van Mulders, G.P. Van Onsem, I. Villella

Université Libre de Bruxelles, Bruxelles, Belgium
O. Charaf, B. Clerbaux, G. De Lentdecker, V. Dero, A.P.R. Gay, G.H. Hammad, T. Hreus, P.E. Marage, A. Raval, L. Thomas, G. Vander Marcken, C. Vander Velde, P. Vanlaer

Ghent University, Ghent, Belgium
V. Adler, A. Cimmino, S. Costantini, M. Grunewald, B. Klein, J. Lellouch, A. Marinov, J. Mccartin, D. Ryckbosch, F. Thyssen, M. Tytgat, L. Vanelderen, P. Verwilligen, S. Walsh, N. Zaganidis

Université Catholique de Louvain, Louvain-la-Neuve, Belgium
S. Basegmez, G. Bruno, J. Caudron, L. Ceard, E. Cortina Gil, J. De Favereau De Jeneret, C. Delaere, D. Favart, A. Giammanco, G. Grégoire, J. Hollar, V. Lemaitre, J. Liao, O. Militaru, C. Nuttens, S. Ovyn, D. Pagano, A. Pin, K. Piotrzkowski, N. Schul

Université de Mons, Mons, Belgium
N. Beliy, T. Caebergs, E. Daubie

Centro Brasileiro de Pesquisas Fisicas, Rio de Janeiro, Brazil
G.A. Alves, L. Brito, D. De Jesus Damiao, M.E. Pol, M.H.G. Souza

Universidade do Estado do Rio de Janeiro, Rio de Janeiro, Brazil
W.L. Aldá Júnior, W. Carvalho, E.M. Da Costa, C. De Oliveira Martins, S. Fonseca De Souza, L. Mundim, H. Nogima, V. Oguri, W.L. Prado Da Silva, A. Santoro, S.M. Silva Do Amaral, A. Sznajder

Instituto de Fisica Teorica, Universidade Estadual Paulista, Sao Paulo, Brazil
C.A. Bernardes[2], F.A. Dias[3], T. Dos Anjos Costa[2], T.R. Fernandez Perez Tomei, E. M. Gregores[2], C. Lagana, F. Marinho, P.G. Mercadante[2], S.F. Novaes, Sandra S. Padula

Institute for Nuclear Research and Nuclear Energy, Sofia, Bulgaria
N. Darmenov[1], V. Genchev[1], P. Iaydjiev[1], S. Piperov, M. Rodozov, S. Stoykova, G. Sultanov, V. Tcholakov, R. Trayanov, M. Vutova

University of Sofia, Sofia, Bulgaria
A. Dimitrov, R. Hadjiiska, A. Karadzhinova, V. Kozhuharov, L. Litov, M. Mateev, B. Pavlov, P. Petkov

Institute of High Energy Physics, Beijing, China
J.G. Bian, G.M. Chen, H.S. Chen, C.H. Jiang, D. Liang, S. Liang, X. Meng, J. Tao, J. Wang, J. Wang, X. Wang, Z. Wang, H. Xiao, M. Xu, J. Zang, Z. Zhang

State Key Lab. of Nucl. Phys. and Tech., Peking University, Beijing, China
Y. Ban, S. Guo, Y. Guo, W. Li, Y. Mao, S.J. Qian, H. Teng, B. Zhu, W. Zou

Universidad de Los Andes, Bogota, Colombia
A. Cabrera, B. Gomez Moreno, A.A. Ocampo Rios, A.F. Osorio Oliveros, J.C. Sanabria

Technical University of Split, Split, Croatia
N. Godinovic, D. Lelas, K. Lelas, R. Plestina[4], D. Polic, I. Puljak

University of Split, Split, Croatia
Z. Antunovic, M. Dzelalija, M. Kovac

Institute Rudjer Boskovic, Zagreb, Croatia
V. Brigljevic, S. Duric, K. Kadija, J. Luetic, S. Morovic

University of Cyprus, Nicosia, Cyprus
A. Attikis, M. Galanti, J. Mousa, C. Nicolaou, F. Ptochos, P.A. Razis

Charles University, Prague, Czech Republic
M. Finger, M. Finger Jr.

Academy of Scientific Research and Technology of the Arab Republic of Egypt, Egyptian Network of High Energy Physics, Cairo, Egypt
Y. Assran[5], A. Ellithi Kamel, S. Khalil[6], M.A. Mahmoud[7], A. Radi[8]

National Institute of Chemical Physics and Biophysics, Tallinn, Estonia
A. Hektor, M. Kadastik, M. Müntel, M. Raidal, L. Rebane, A. Tiko

Department of Physics, University of Helsinki, Helsinki, Finland
V. Azzolini, P. Eerola, G. Fedi, M. Voutilainen

Helsinki Institute of Physics, Helsinki, Finland
S. Czellar, J. Härkönen, A. Heikkinen, V. Karimäki, R. Kinnunen, M.J. Kortelainen, T. Lampén, K. Lassila-Perini, S. Lehti, T. Lindén, P. Luukka, T. Mäenpää, E. Tuominen, J. Tuominiemi, E. Tuovinen, D. Ungaro, L. Wendland

Lappeenranta University of Technology, Lappeenranta, Finland
K. Banzuzi, A. Karjalainen, A. Korpela, T. Tuuva

Laboratoire d'Annecy-le-Vieux de Physique des Particules, IN2P3-CNRS, Annecy-le-Vieux, France
D. Sillou

DSM/IRFU, CEA/Saclay, Gif-sur-Yvette, France
M. Besancon, S. Choudhury, M. Dejardin, D. Denegri, B. Fabbro, J.L. Faure, F. Ferri, S. Ganjour, F.X. Gentit, A. Givernaud, P. Gras, G. Hamel de Monchenault, P. Jarry, E. Locci, J. Malcles, M. Marionneau, L. Millischer, J. Rander, A. Rosowsky, I. Shreyber, M. Titov, P. Verrecchia

Laboratoire Leprince-Ringuet, Ecole Polytechnique, IN2P3-CNRS, Palaiseau, France
S. Baffioni, F. Beaudette, L. Benhabib, L. Bianchini, M. Bluj[9], C. Broutin, P. Busson, C. Charlot, T. Dahms, L. Dobrzynski, S. Elgammal, R. Granier de Cassagnac, M. Haguenauer, P. Miné, C. Mironov, C. Ochando, P. Paganini, D. Sabes, R. Salerno, Y. Sirois, C. Thiebaux, B. Wyslouch[10], A. Zabi

Institut Pluridisciplinaire Hubert Curien, Université de Strasbourg, Université de Haute Alsace Mulhouse, CNRS/IN2P3, Strasbourg, France
J.-L. Agram[11], J. Andrea, D. Bloch, D. Bodin, J.-M. Brom, M. Cardaci, E.C. Chabert, C. Collard, E. Conte[11], F. Drouhin[11], C. Ferro, J.-C. Fontaine[11], D. Gelé, U. Goerlach, S. Greder, P. Juillot, M. Karim[11], A.-C. Le Bihan, Y. Mikami, P. Van Hove

Centre de Calcul de l'Institut National de Physique Nucleaire et de Physique des Particules (IN2P3), Villeurbanne, France
F. Fassi, D. Mercier

Université de Lyon, Université Claude Bernard Lyon 1, CNRS-IN2P3, Institut de Physique Nucléaire de Lyon, Villeurbanne, France
C. Baty, S. Beauceron, N. Beaupere, M. Bedjidian, O. Bondu, G. Boudoul, D. Boumediene, H. Brun, J. Chasserat, R. Chierici, D. Contardo, P. Depasse, H. El Mamouni, J. Fay, S. Gascon, B. Ille, T. Kurca, T. Le Grand, M. Lethuillier, L. Mirabito, S. Perries, V. Sordini, S. Tosi, Y. Tschudi, P. Verdier, S. Viret

Institute of High Energy Physics and Informatization, Tbilisi State University, Tbilisi, Georgia
D. Lomidze

RWTH Aachen University, I. Physikalisches Institut, Aachen, Germany
G. Anagnostou, S. Beranek, M. Edelhoff, L. Feld, N. Heracleous, O. Hindrichs, R. Jussen, K. Klein, J. Merz, N. Mohr, A. Ostapchuk, A. Perieanu, F. Raupach, J. Sammet, S. Schael, D. Sprenger, H. Weber, M. Weber, B. Wittmer, V. Zhukov[12]

RWTH Aachen University, III. Physikalisches Institut A, Aachen, Germany
M. Ata, E. Dietz-Laursonn, M. Erdmann, T. Hebbeker, C. Heidemann, A. Hinzmann, K. Hoepfner, T. Klimkovich, D. Klingebiel, P. Kreuzer, D. Lanske†, J. Lingemann, C. Magass, M. Merschmeyer, A. Meyer, P. Papacz, H. Pieta, H. Reithler, S.A. Schmitz, L. Sonnenschein, J. Steggemann, D. Teyssier

RWTH Aachen University, III. Physikalisches Institut B, Aachen, Germany
M. Bontenackels, V. Cherepanov, M. Davids, G. Flügge, H. Geenen, M. Giffels, W. Haj Ahmad, F. Hoehle, B. Kargoll, T. Kress, Y. Kuessel, A. Linn, A. Nowack, L. Perchalla, O. Pooth, J. Rennefeld, P. Sauerland, A. Stahl, D. Tornier, M.H. Zoeller

Deutsches Elektronen-Synchrotron, Hamburg, Germany
M. Aldaya Martin, W. Behrenhoff, U. Behrens, M. Bergholz[13], A. Bethani, K. Borras, A. Cakir, A. Campbell, E. Castro, D. Dammann, G. Eckerlin, D. Eckstein, A. Flossdorf, G. Flucke, A. Geiser, J. Hauk, H. Jung[1], M. Kasemann, P. Katsas, C. Kleinwort, H. Kluge, A. Knutsson, M. Krämer, D. Krücker, E. Kuznetsova, W. Lange, W. Lohmann[13], R. Mankel, M. Marienfeld, I.-A. Melzer-Pellmann, A.B. Meyer, J. Mnich, A. Mussgiller, J. Olzem, A. Petrukhin, D. Pitzl, A. Raspereza, M. Rosin, R. Schmidt[13], T. Schoerner-Sadenius, N. Sen, A. Spiridonov, M. Stein, J. Tomaszewska, R. Walsh, C. Wissing

University of Hamburg, Hamburg, Germany
C. Autermann, V. Blobel, S. Bobrovskyi, J. Draeger, H. Enderle, U. Gebbert, M. Görner,

T. Hermanns, K. Kaschube, G. Kaussen, H. Kirschenmann, R. Klanner, J. Lange, B. Mura, S. Naumann-Emme, F. Nowak, N. Pietsch, C. Sander, H. Schettler, P. Schleper, E. Schlieckau, M. Schröder, T. Schum, H. Stadie, G. Steinbrück, J. Thomsen

Institut für Experimentelle Kernphysik, Karlsruhe, Germany
C. Barth, J. Bauer, J. Berger, V. Buege, T. Chwalek, W. De Boer, A. Dierlamm, G. Dirkes, M. Feindt, J. Gruschke, C. Hackstein, F. Hartmann, M. Heinrich, H. Held, K.H. Hoffmann, S. Honc, I. Katkov[12], J.R. Komaragiri, T. Kuhr, D. Martschei, S. Mueller, Th. Müller, M. Niegel, O. Oberst, A. Oehler, J. Ott, T. Peiffer, G. Quast, K. Rabbertz, F. Ratnikov, N. Ratnikova, M. Renz, S. Röcker, C. Saout, A. Scheurer, P. Schieferdecker, F.-P. Schilling, M. Schmanau, G. Schott, H.J. Simonis, F.M. Stober, D. Troendle, J. Wagner-Kuhr, T. Weiler, M. Zeise, E.B. Ziebarth

Institute of Nuclear Physics "Demokritos", Aghia Paraskevi, Greece
G. Daskalakis, T. Geralis, S. Kesisoglou, A. Kyriakis, D. Loukas, I. Manolakos, A. Markou, C. Markou, C. Mavrommatis, E. Ntomari, E. Petrakou

University of Athens, Athens, Greece
L. Gouskos, T.J. Mertzimekis, A. Panagiotou, N. Saoulidou, E. Stiliaris

University of Ioánnina, Ioánnina, Greece
I. Evangelou, C. Foudas[1], P. Kokkas, N. Manthos, I. Papadopoulos, V. Patras, F.A. Triantis

KFKI Research Institute for Particle and Nuclear Physics, Budapest, Hungary
A. Aranyi, G. Bencze, L. Boldizsar, C. Hajdu[1], P. Hidas, D. Horvath[14], A. Kapusi, K. Krajczar[15], F. Sikler[1], G.I. Veres[15], G. Vesztergombi[15]

Institute of Nuclear Research ATOMKI, Debrecen, Hungary
N. Beni, J. Molnar, J. Palinkas, Z. Szillasi, V. Veszpremi

University of Debrecen, Debrecen, Hungary
P. Raics, Z.L. Trocsanyi, B. Ujvari

Panjab University, Chandigarh, India
S.B. Beri, V. Bhatnagar, N. Dhingra, R. Gupta, M. Jindal, M. Kaur, J.M. Kohli, M.Z. Mehta, N. Nishu, L.K. Saini, A. Sharma, A.P. Singh, J. Singh, S.P. Singh

University of Delhi, Delhi, India
S. Ahuja, B.C. Choudhary, P. Gupta, A. Kumar, A. Kumar, S. Malhotra, M. Naimuddin, K. Ranjan, R.K. Shivpuri

Saha Institute of Nuclear Physics, Kolkata, India
S. Banerjee, S. Bhattacharya, S. Dutta, B. Gomber, S. Jain, S. Jain, R. Khurana, S. Sarkar

Bhabha Atomic Research Centre, Mumbai, India
R.K. Choudhury, D. Dutta, S. Kailas, V. Kumar, P. Mehta, A.K. Mohanty[1], L.M. Pant, P. Shukla

Tata Institute of Fundamental Research - EHEP, Mumbai, India
T. Aziz, M. Guchait[16], A. Gurtu, M. Maity[17], D. Majumder, G. Majumder, T. Mathew, K. Mazumdar, G.B. Mohanty, A. Saha, K. Sudhakar, N. Wickramage

Tata Institute of Fundamental Research - HECR, Mumbai, India
S. Banerjee, S. Dugad, N.K. Mondal

Institute for Research and Fundamental Sciences (IPM), Tehran, Iran
H. Arfaei, H. Bakhshiansohi[18], S.M. Etesami[19], A. Fahim[18], M. Hashemi, H. Hesari, A. Jafari[18],

M. Khakzad, A. Mohammadi[20], M. Mohammadi Najafabadi, S. Paktinat Mehdiabadi, B. Safarzadeh, M. Zeinali[19]

INFN Sezione di Bari [a], Università di Bari [b], Politecnico di Bari [c], Bari, Italy
M. Abbrescia[a,b], L. Barbone[a,b], C. Calabria[a,b], A. Colaleo[a], D. Creanza[a,c], N. De Filippis[a,c,1], M. De Palma[a,b], L. Fiore[a], G. Iaselli[a,c], L. Lusito[a,b], G. Maggi[a,c], M. Maggi[a], N. Manna[a,b], B. Marangelli[a,b], S. My[a,c], S. Nuzzo[a,b], N. Pacifico[a,b], G.A. Pierro[a], A. Pompili[a,b], G. Pugliese[a,c], F. Romano[a,c], G. Roselli[a,b], G. Selvaggi[a,b], L. Silvestris[a], R. Trentadue[a], S. Tupputi[a,b], G. Zito[a]

INFN Sezione di Bologna [a], Università di Bologna [b], Bologna, Italy
G. Abbiendi[a], A.C. Benvenuti[a], D. Bonacorsi[a], S. Braibant-Giacomelli[a,b], L. Brigliadori[a], P. Capiluppi[a,b], A. Castro[a,b], F.R. Cavallo[a], M. Cuffiani[a,b], G.M. Dallavalle[a], F. Fabbri[a], A. Fanfani[a,b], D. Fasanella[a,1], P. Giacomelli[a], M. Giunta[a], C. Grandi[a], S. Marcellini[a], G. Masetti[b], M. Meneghelli[a,b], A. Montanari[a], F.L. Navarria[a,b], F. Odorici[a], A. Perrotta[a], F. Primavera[a], A.M. Rossi[a,b], T. Rovelli[a,b], G. Siroli[a,b], R. Travaglini[a,b]

INFN Sezione di Catania [a], Università di Catania [b], Catania, Italy
S. Albergo[a,b], G. Cappello[a,b], M. Chiorboli[a,b], S. Costa[a,b], R. Potenza[a,b], A. Tricomi[a,b], C. Tuve[a,b]

INFN Sezione di Firenze [a], Università di Firenze [b], Firenze, Italy
G. Barbagli[a], V. Ciulli[a,b], C. Civinini[a], R. D'Alessandro[a,b], E. Focardi[a,b], S. Frosali[a,b], E. Gallo[a], S. Gonzi[a,b], P. Lenzi[a,b], M. Meschini[a], S. Paoletti[a], G. Sguazzoni[a], A. Tropiano[a,1]

INFN Laboratori Nazionali di Frascati, Frascati, Italy
L. Benussi, S. Bianco, S. Colafranceschi[21], F. Fabbri, D. Piccolo

INFN Sezione di Genova, Genova, Italy
P. Fabbricatore, R. Musenich

INFN Sezione di Milano-Bicocca [a], Università di Milano-Bicocca [b], Milano, Italy
A. Benaglia[a,b,1], F. De Guio[a,b], L. Di Matteo[a,b], S. Gennai[1], A. Ghezzi[a,b], S. Malvezzi[a], A. Martelli[a,b], A. Massironi[a,b,1], D. Menasce[a], L. Moroni[a], M. Paganoni[a,b], D. Pedrini[a], S. Ragazzi[a,b], N. Redaelli[a], S. Sala[a], T. Tabarelli de Fatis[a,b]

INFN Sezione di Napoli [a], Università di Napoli "Federico II" [b], Napoli, Italy
S. Buontempo[a], C.A. Carrillo Montoya[a,1], N. Cavallo[a,22], A. De Cosa[a,b], F. Fabozzi[a,22], A.O.M. Iorio[a,1], L. Lista[a], M. Merola[a,b], P. Paolucci[a]

INFN Sezione di Padova [a], Università di Padova [b], Università di Trento (Trento) [c], Padova, Italy
P. Azzi[a], N. Bacchetta[a,1], P. Bellan[a,b], D. Bisello[a,b], A. Branca[a], R. Carlin[a,b], P. Checchia[a], T. Dorigo[a], U. Dosselli[a], F. Fanzago[a], F. Gasparini[a,b], U. Gasparini[a,b], A. Gozzelino, S. Lacaprara[a,23], I. Lazzizzera[a,c], M. Margoni[a,b], M. Mazzucato[a], A.T. Meneguzzo[a,b], M. Nespolo[a,1], L. Perrozzi[a], N. Pozzobon[a,b], P. Ronchese[a,b], F. Simonetto[a,b], E. Torassa[a], M. Tosi[a,b,1], S. Vanini[a,b], P. Zotto[a,b], G. Zumerle[a,b]

INFN Sezione di Pavia [a], Università di Pavia [b], Pavia, Italy
P. Baesso[a,b], U. Berzano[a], S.P. Ratti[a,b], C. Riccardi[a,b], P. Torre[a,b], P. Vitulo[a,b], C. Viviani[a,b]

INFN Sezione di Perugia [a], Università di Perugia [b], Perugia, Italy
M. Biasini[a,b], G.M. Bilei[a], B. Caponeri[a,b], L. Fanò[a,b], P. Lariccia[a,b], A. Lucaroni[a,b,1], G. Mantovani[a,b], M. Menichelli[a], A. Nappi[a,b], F. Romeo[a,b], A. Santocchia[a,b], S. Taroni[a,b,1], M. Valdata[a,b]

INFN Sezione di Pisa [a], Università di Pisa [b], Scuola Normale Superiore di Pisa [c], Pisa, Italy
P. Azzurri[a,c], G. Bagliesi[a], J. Bernardini[a,b], T. Boccali[a], G. Broccolo[a,c], R. Castaldi[a], R.T. D'Agnolo[a,c], R. Dell'Orso[a], F. Fiori[a,b], L. Foà[a,c], A. Giassi[a], A. Kraan[a], F. Ligabue[a,c], T. Lomtadze[a], L. Martini[a,24], A. Messineo[a,b], F. Palla[a], F. Palmonari, G. Segneri[a], A.T. Serban[a], P. Spagnolo[a], R. Tenchini[a], G. Tonelli[a,b,1], A. Venturi[a,1], P.G. Verdini[a]

INFN Sezione di Roma [a], Università di Roma "La Sapienza" [b], Roma, Italy
L. Barone[a,b], F. Cavallari[a], D. Del Re[a,b,1], E. Di Marco[a,b], M. Diemoz[a], D. Franci[a,b], M. Grassi[a,1], E. Longo[a,b], P. Meridiani, S. Nourbakhsh[a], G. Organtini[a,b], F. Pandolfi[a,b], R. Paramatti[a], S. Rahatlou[a,b], M. Sigamani[a]

INFN Sezione di Torino [a], Università di Torino [b], Università del Piemonte Orientale (Novara) [c], Torino, Italy
N. Amapane[a,b], R. Arcidiacono[a,c], S. Argiro[a,b], M. Arneodo[a,c], C. Biino[a], C. Botta[a,b], N. Cartiglia[a], R. Castello[a,b], M. Costa[a,b], N. Demaria[a], A. Graziano[a,b], C. Mariotti[a], S. Maselli[a], E. Migliore[a,b], V. Monaco[a,b], M. Musich[a], M.M. Obertino[a,c], N. Pastrone[a], M. Pelliccioni[a,b], A. Potenza[a,b], A. Romero[a,b], M. Ruspa[a,c], R. Sacchi[a,b], V. Sola[a,b], A. Solano[a,b], A. Staiano[a], A. Vilela Pereira[a]

INFN Sezione di Trieste [a], Università di Trieste [b], Trieste, Italy
S. Belforte[a], F. Cossutti[a], G. Della Ricca[a,b], B. Gobbo[a], M. Marone[a,b], D. Montanino[a,b], A. Penzo[a]

Kangwon National University, Chunchon, Korea
S.G. Heo, S.K. Nam

Kyungpook National University, Daegu, Korea
S. Chang, J. Chung, D.H. Kim, G.N. Kim, J.E. Kim, D.J. Kong, H. Park, S.R. Ro, D.C. Son, T. Son

Chonnam National University, Institute for Universe and Elementary Particles, Kwangju, Korea
Zero Kim, J.Y. Kim, S. Song

Konkuk University, Seoul, Korea
H.Y. Jo

Korea University, Seoul, Korea
S. Choi, D. Gyun, B. Hong, M. Jo, H. Kim, J.H. Kim, T.J. Kim, K.S. Lee, D.H. Moon, S.K. Park, E. Seo, K.S. Sim

University of Seoul, Seoul, Korea
M. Choi, S. Kang, H. Kim, C. Park, I.C. Park, S. Park, G. Ryu

Sungkyunkwan University, Suwon, Korea
Y. Cho, Y. Choi, Y.K. Choi, J. Goh, M.S. Kim, B. Lee, J. Lee, S. Lee, H. Seo, I. Yu

Vilnius University, Vilnius, Lithuania
M.J. Bilinskas, I. Grigelionis, M. Janulis, D. Martisiute, P. Petrov, M. Polujanskas, T. Sabonis

Centro de Investigacion y de Estudios Avanzados del IPN, Mexico City, Mexico
H. Castilla-Valdez, E. De La Cruz-Burelo, I. Heredia-de La Cruz, R. Lopez-Fernandez, R. Magaña Villalba, J. Martínez-Ortega, A. Sánchez-Hernández, L.M. Villasenor-Cendejas

Universidad Iberoamericana, Mexico City, Mexico
S. Carrillo Moreno, F. Vazquez Valencia

Benemerita Universidad Autonoma de Puebla, Puebla, Mexico
H.A. Salazar Ibarguen

Universidad Autónoma de San Luis Potosí, San Luis Potosí, Mexico
E. Casimiro Linares, A. Morelos Pineda, M.A. Reyes-Santos

University of Auckland, Auckland, New Zealand
D. Krofcheck, J. Tam

University of Canterbury, Christchurch, New Zealand
P.H. Butler, R. Doesburg, H. Silverwood

National Centre for Physics, Quaid-I-Azam University, Islamabad, Pakistan
M. Ahmad, I. Ahmed, M.H. Ansari, M.I. Asghar, H.R. Hoorani, S. Khalid, W.A. Khan, T. Khurshid, S. Qazi, M.A. Shah, M. Shoaib

Institute of Experimental Physics, Faculty of Physics, University of Warsaw, Warsaw, Poland
G. Brona, M. Cwiok, W. Dominik, K. Doroba, A. Kalinowski, M. Konecki, J. Krolikowski

Soltan Institute for Nuclear Studies, Warsaw, Poland
T. Frueboes, R. Gokieli, M. Górski, M. Kazana, K. Nawrocki, K. Romanowska-Rybinska, M. Szleper, G. Wrochna, P. Zalewski

Laboratório de Instrumentação e Física Experimental de Partículas, Lisboa, Portugal
N. Almeida, P. Bargassa, A. David, P. Faccioli, P.G. Ferreira Parracho, M. Gallinaro[1], P. Musella, A. Nayak, J. Pela[1], P.Q. Ribeiro, J. Seixas, J. Varela

Joint Institute for Nuclear Research, Dubna, Russia
S. Afanasiev, I. Belotelov, P. Bunin, M. Gavrilenko, I. Golutvin, A. Kamenev, V. Karjavin, G. Kozlov, A. Lanev, P. Moisenz, V. Palichik, V. Perelygin, S. Shmatov, V. Smirnov, A. Volodko, A. Zarubin

Petersburg Nuclear Physics Institute, Gatchina (St Petersburg), Russia
V. Golovtsov, Y. Ivanov, V. Kim, P. Levchenko, V. Murzin, V. Oreshkin, I. Smirnov, V. Sulimov, L. Uvarov, S. Vavilov, A. Vorobyev, An. Vorobyev

Institute for Nuclear Research, Moscow, Russia
Yu. Andreev, A. Dermenev, S. Gninenko, N. Golubev, M. Kirsanov, N. Krasnikov, V. Matveev, A. Pashenkov, A. Toropin, S. Troitsky

Institute for Theoretical and Experimental Physics, Moscow, Russia
V. Epshteyn, M. Erofeeva, V. Gavrilov, V. Kaftanov†, M. Kossov[1], A. Krokhotin, N. Lychkovskaya, V. Popov, G. Safronov, S. Semenov, V. Stolin, E. Vlasov, A. Zhokin

Moscow State University, Moscow, Russia
A. Belyaev, E. Boos, M. Dubinin[3], L. Dudko, A. Ershov, A. Gribushin, O. Kodolova, I. Lokhtin, A. Markina, S. Obraztsov, M. Perfilov, S. Petrushanko, L. Sarycheva, V. Savrin, A. Snigirev

P.N. Lebedev Physical Institute, Moscow, Russia
V. Andreev, M. Azarkin, I. Dremin, M. Kirakosyan, A. Leonidov, G. Mesyats, S.V. Rusakov, A. Vinogradov

State Research Center of Russian Federation, Institute for High Energy Physics, Protvino, Russia
I. Azhgirey, I. Bayshev, S. Bitioukov, V. Grishin[1], V. Kachanov, D. Konstantinov, A. Korablev,

V. Krychkine, V. Petrov, R. Ryutin, A. Sobol, L. Tourtchanovitch, S. Troshin, N. Tyurin, A. Uzunian, A. Volkov

University of Belgrade, Faculty of Physics and Vinca Institute of Nuclear Sciences, Belgrade, Serbia
P. Adzic[25], M. Djordjevic, D. Krpic[25], J. Milosevic

Centro de Investigaciones Energéticas Medioambientales y Tecnológicas (CIEMAT), Madrid, Spain
M. Aguilar-Benitez, J. Alcaraz Maestre, P. Arce, C. Battilana, E. Calvo, M. Cerrada, M. Chamizo Llatas, N. Colino, B. De La Cruz, A. Delgado Peris, C. Diez Pardos, D. Domínguez Vázquez, C. Fernandez Bedoya, J.P. Fernández Ramos, A. Ferrando, J. Flix, M.C. Fouz, P. Garcia-Abia, O. Gonzalez Lopez, S. Goy Lopez, J.M. Hernandez, M.I. Josa, G. Merino, J. Puerta Pelayo, I. Redondo, L. Romero, J. Santaolalla, M.S. Soares, C. Willmott

Universidad Autónoma de Madrid, Madrid, Spain
C. Albajar, G. Codispoti, J.F. de Trocóniz

Universidad de Oviedo, Oviedo, Spain
J. Cuevas, J. Fernandez Menendez, S. Folgueras, I. Gonzalez Caballero, L. Lloret Iglesias, J.M. Vizan Garcia

Instituto de Física de Cantabria (IFCA), CSIC-Universidad de Cantabria, Santander, Spain
J.A. Brochero Cifuentes, I.J. Cabrillo, A. Calderon, S.H. Chuang, J. Duarte Campderros, M. Felcini[26], M. Fernandez, G. Gomez, J. Gonzalez Sanchez, C. Jorda, P. Lobelle Pardo, A. Lopez Virto, J. Marco, R. Marco, C. Martinez Rivero, F. Matorras, F.J. Munoz Sanchez, J. Piedra Gomez[27], T. Rodrigo, A.Y. Rodríguez-Marrero, A. Ruiz-Jimeno, L. Scodellaro, M. Sobron Sanudo, I. Vila, R. Vilar Cortabitarte

CERN, European Organization for Nuclear Research, Geneva, Switzerland
D. Abbaneo, E. Auffray, G. Auzinger, P. Baillon, A.H. Ball, D. Barney, A.J. Bell[28], D. Benedetti, C. Bernet[4], W. Bialas, P. Bloch, A. Bocci, S. Bolognesi, M. Bona, H. Breuker, K. Bunkowski, T. Camporesi, G. Cerminara, T. Christiansen, J.A. Coarasa Perez, B. Curé, D. D'Enterria, A. De Roeck, S. Di Guida, N. Dupont-Sagorin, A. Elliott-Peisert, B. Frisch, W. Funk, A. Gaddi, G. Georgiou, H. Gerwig, D. Gigi, K. Gill, D. Giordano, F. Glege, R. Gomez-Reino Garrido, M. Gouzevitch, P. Govoni, S. Gowdy, R. Guida, L. Guiducci, M. Hansen, C. Hartl, J. Harvey, J. Hegeman, B. Hegner, H.F. Hoffmann, V. Innocente, P. Janot, K. Kaadze, E. Karavakis, P. Lecoq, C. Lourenço, T. Mäki, M. Malberti, L. Malgeri, M. Mannelli, L. Masetti, A. Maurisset, F. Meijers, S. Mersi, E. Meschi, R. Moser, M.U. Mozer, M. Mulders, E. Nesvold, M. Nguyen, T. Orimoto, L. Orsini, E. Palencia Cortezon, E. Perez, A. Petrilli, A. Pfeiffer, M. Pierini, M. Pimiä, D. Piparo, G. Polese, L. Quertenmont, A. Racz, W. Reece, J. Rodrigues Antunes, G. Rolandi[29], T. Rommerskirchen, C. Rovelli[30], M. Rovere, H. Sakulin, C. Schäfer, C. Schwick, I. Segoni, A. Sharma, P. Siegrist, P. Silva, M. Simon, P. Sphicas[31], D. Spiga, M. Spiropulu[3], M. Stoye, A. Tsirou, P. Vichoudis, H.K. Wöhri, S.D. Worm, W.D. Zeuner

Paul Scherrer Institut, Villigen, Switzerland
W. Bertl, K. Deiters, W. Erdmann, K. Gabathuler, R. Horisberger, Q. Ingram, H.C. Kaestli, S. König, D. Kotlinski, U. Langenegger, F. Meier, D. Renker, T. Rohe, J. Sibille[32]

Institute for Particle Physics, ETH Zurich, Zurich, Switzerland
L. Bäni, P. Bortignon, L. Caminada[33], B. Casal, N. Chanon, Z. Chen, S. Cittolin, G. Dissertori, M. Dittmar, J. Eugster, K. Freudenreich, C. Grab, W. Hintz, P. Lecomte, W. Lustermann, C. Marchica[33], P. Martinez Ruiz del Arbol, P. Milenovic[34], F. Moortgat, C. Nägeli[33], P. Nef,

F. Nessi-Tedaldi, L. Pape, F. Pauss, T. Punz, A. Rizzi, F.J. Ronga, M. Rossini, L. Sala, A.K. Sanchez, M.-C. Sawley, A. Starodumov[35], B. Stieger, M. Takahashi, L. Tauscher†, A. Thea, K. Theofilatos, D. Treille, C. Urscheler, R. Wallny, M. Weber, L. Wehrli, J. Weng

Universität Zürich, Zurich, Switzerland
E. Aguilo, C. Amsler, V. Chiochia, S. De Visscher, C. Favaro, M. Ivova Rikova, A. Jaeger, B. Millan Mejias, P. Otiougova, P. Robmann, A. Schmidt, H. Snoek

National Central University, Chung-Li, Taiwan
Y.H. Chang, K.H. Chen, C.M. Kuo, S.W. Li, W. Lin, Z.K. Liu, Y.J. Lu, D. Mekterovic, R. Volpe, S.S. Yu

National Taiwan University (NTU), Taipei, Taiwan
P. Bartalini, P. Chang, Y.H. Chang, Y.W. Chang, Y. Chao, K.F. Chen, W.-S. Hou, Y. Hsiung, K.Y. Kao, Y.J. Lei, R.-S. Lu, J.G. Shiu, Y.M. Tzeng, X. Wan, M. Wang

Cukurova University, Adana, Turkey
A. Adiguzel, M.N. Bakirci[36], S. Cerci[37], C. Dozen, I. Dumanoglu, E. Eskut, S. Girgis, G. Gokbulut, I. Hos, E.E. Kangal, A. Kayis Topaksu, G. Onengut, K. Ozdemir, S. Ozturk[38], A. Polatoz, K. Sogut[39], D. Sunar Cerci[37], B. Tali[37], H. Topakli[36], D. Uzun, L.N. Vergili, M. Vergili

Middle East Technical University, Physics Department, Ankara, Turkey
I.V. Akin, T. Aliev, B. Bilin, S. Bilmis, M. Deniz, H. Gamsizkan, A.M. Guler, K. Ocalan, A. Ozpineci, M. Serin, R. Sever, U.E. Surat, M. Yalvac, E. Yildirim, M. Zeyrek

Bogazici University, Istanbul, Turkey
M. Deliomeroglu, D. Demir[40], E. Gülmez, B. Isildak, M. Kaya[41], O. Kaya[41], M. Özbek, S. Ozkorucuklu[42], N. Sonmez[43]

National Scientific Center, Kharkov Institute of Physics and Technology, Kharkov, Ukraine
L. Levchuk

University of Bristol, Bristol, United Kingdom
F. Bostock, J.J. Brooke, T.L. Cheng, E. Clement, D. Cussans, R. Frazier, J. Goldstein, M. Grimes, D. Hartley, G.P. Heath, H.F. Heath, L. Kreczko, S. Metson, D.M. Newbold[44], K. Nirunpong, A. Poll, S. Senkin, V.J. Smith

Rutherford Appleton Laboratory, Didcot, United Kingdom
L. Basso[45], K.W. Bell, A. Belyaev[45], C. Brew, R.M. Brown, B. Camanzi, D.J.A. Cockerill, J.A. Coughlan, K. Harder, S. Harper, J. Jackson, B.W. Kennedy, E. Olaiya, D. Petyt, B.C. Radburn-Smith, C.H. Shepherd-Themistocleous, I.R. Tomalin, W.J. Womersley

Imperial College, London, United Kingdom
R. Bainbridge, G. Ball, J. Ballin, R. Beuselinck, O. Buchmuller, D. Colling, N. Cripps, M. Cutajar, G. Davies, M. Della Negra, W. Ferguson, J. Fulcher, D. Futyan, A. Gilbert, A. Guneratne Bryer, G. Hall, Z. Hatherell, J. Hays, G. Iles, M. Jarvis, G. Karapostoli, L. Lyons, B.C. MacEvoy, A.-M. Magnan, J. Marrouche, B. Mathias, R. Nandi, J. Nash, A. Nikitenko[35], A. Papageorgiou, M. Pesaresi, K. Petridis, M. Pioppi[46], D.M. Raymond, S. Rogerson, N. Rompotis, A. Rose, M.J. Ryan, C. Seez, P. Sharp, A. Sparrow, A. Tapper, S. Tourneur, M. Vazquez Acosta, T. Virdee, S. Wakefield, N. Wardle, D. Wardrope, T. Whyntie

Brunel University, Uxbridge, United Kingdom
M. Barrett, M. Chadwick, J.E. Cole, P.R. Hobson, A. Khan, P. Kyberd, D. Leslie, W. Martin, I.D. Reid, L. Teodorescu

Baylor University, Waco, USA
K. Hatakeyama, H. Liu

The University of Alabama, Tuscaloosa, USA
C. Henderson

Boston University, Boston, USA
T. Bose, E. Carrera Jarrin, C. Fantasia, A. Heister, J. St. John, P. Lawson, D. Lazic, J. Rohlf, D. Sperka, L. Sulak

Brown University, Providence, USA
A. Avetisyan, S. Bhattacharya, J.P. Chou, D. Cutts, A. Ferapontov, U. Heintz, S. Jabeen, G. Kukartsev, G. Landsberg, M. Luk, M. Narain, D. Nguyen, M. Segala, T. Sinthuprasith, T. Speer, K.V. Tsang

University of California, Davis, Davis, USA
R. Breedon, G. Breto, M. Calderon De La Barca Sanchez, S. Chauhan, M. Chertok, J. Conway, R. Conway, P.T. Cox, J. Dolen, R. Erbacher, E. Friis, R. Houtz, W. Ko, A. Kopecky, R. Lander, H. Liu, O. Mall, S. Maruyama, T. Miceli, M. Nikolic, D. Pellett, J. Robles, B. Rutherford, S. Salur, T. Schwarz, M. Searle, J. Smith, M. Squires, M. Tripathi, R. Vasquez Sierra, C. Veelken

University of California, Los Angeles, Los Angeles, USA
V. Andreev, K. Arisaka, D. Cline, R. Cousins, A. Deisher, J. Duris, S. Erhan, C. Farrell, J. Hauser, M. Ignatenko, C. Jarvis, C. Plager, G. Rakness, P. Schlein†, J. Tucker, V. Valuev

University of California, Riverside, Riverside, USA
J. Babb, R. Clare, J. Ellison, J.W. Gary, F. Giordano, G. Hanson, G.Y. Jeng, S.C. Kao, H. Liu, O.R. Long, A. Luthra, H. Nguyen, S. Paramesvaran, B.C. Shen†, R. Stringer, J. Sturdy, S. Sumowidagdo, R. Wilken, S. Wimpenny

University of California, San Diego, La Jolla, USA
W. Andrews, J.G. Branson, G.B. Cerati, D. Evans, F. Golf, A. Holzner, R. Kelley, M. Lebourgeois, J. Letts, B. Mangano, S. Padhi, C. Palmer, G. Petrucciani, H. Pi, M. Pieri, R. Ranieri, M. Sani, V. Sharma, S. Simon, E. Sudano, M. Tadel, Y. Tu, A. Vartak, S. Wasserbaech[47], F. Würthwein, A. Yagil, J. Yoo

University of California, Santa Barbara, Santa Barbara, USA
D. Barge, R. Bellan, C. Campagnari, M. D'Alfonso, T. Danielson, K. Flowers, P. Geffert, J. Incandela, C. Justus, P. Kalavase, S.A. Koay, D. Kovalskyi[1], V. Krutelyov, S. Lowette, N. Mccoll, S.D. Mullin, V. Pavlunin, F. Rebassoo, J. Ribnik, J. Richman, R. Rossin, D. Stuart, W. To, J.R. Vlimant, C. West

California Institute of Technology, Pasadena, USA
A. Apresyan, A. Bornheim, J. Bunn, Y. Chen, M. Gataullin, Y. Ma, A. Mott, H.B. Newman, C. Rogan, K. Shin, V. Timciuc, P. Traczyk, J. Veverka, R. Wilkinson, Y. Yang, R.Y. Zhu

Carnegie Mellon University, Pittsburgh, USA
B. Akgun, R. Carroll, T. Ferguson, Y. Iiyama, D.W. Jang, S.Y. Jun, Y.F. Liu, M. Paulini, J. Russ, H. Vogel, I. Vorobiev

University of Colorado at Boulder, Boulder, USA
J.P. Cumalat, M.E. Dinardo, B.R. Drell, C.J. Edelmaier, W.T. Ford, A. Gaz, B. Heyburn, E. Luiggi Lopez, U. Nauenberg, J.G. Smith, K. Stenson, K.A. Ulmer, S.R. Wagner, S.L. Zang

Cornell University, Ithaca, USA
L. Agostino, J. Alexander, A. Chatterjee, N. Eggert, L.K. Gibbons, B. Heltsley, K. Henriksson, W. Hopkins, A. Khukhunaishvili, B. Kreis, Y. Liu, G. Nicolas Kaufman, J.R. Patterson, D. Puigh, A. Ryd, M. Saelim, E. Salvati, X. Shi, W. Sun, W.D. Teo, J. Thom, J. Thompson, J. Vaughan, Y. Weng, L. Winstrom, P. Wittich

Fairfield University, Fairfield, USA
A. Biselli, G. Cirino, D. Winn

Fermi National Accelerator Laboratory, Batavia, USA
S. Abdullin, M. Albrow, J. Anderson, G. Apollinari, M. Atac, J.A. Bakken, L.A.T. Bauerdick, A. Beretvas, J. Berryhill, P.C. Bhat, I. Bloch, K. Burkett, J.N. Butler, V. Chetluru, H.W.K. Cheung, F. Chlebana, S. Cihangir, W. Cooper, D.P. Eartly, V.D. Elvira, S. Esen, I. Fisk, J. Freeman, Y. Gao, E. Gottschalk, D. Green, K. Gunthoti, O. Gutsche, J. Hanlon, R.M. Harris, J. Hirschauer, B. Hooberman, H. Jensen, S. Jindariani, M. Johnson, U. Joshi, R. Khatiwada, B. Klima, K. Kousouris, S. Kunori, S. Kwan, C. Leonidopoulos, P. Limon, D. Lincoln, R. Lipton, J. Lykken, K. Maeshima, J.M. Marraffino, D. Mason, P. McBride, T. Miao, K. Mishra, S. Mrenna, Y. Musienko[48], C. Newman-Holmes, V. O'Dell, J. Pivarski, R. Pordes, O. Prokofyev, E. Sexton-Kennedy, S. Sharma, W.J. Spalding, L. Spiegel, P. Tan, L. Taylor, S. Tkaczyk, L. Uplegger, E.W. Vaandering, R. Vidal, J. Whitmore, W. Wu, F. Yang, F. Yumiceva, J.C. Yun

University of Florida, Gainesville, USA
D. Acosta, P. Avery, D. Bourilkov, M. Chen, S. Das, M. De Gruttola, G.P. Di Giovanni, D. Dobur, A. Drozdetskiy, R.D. Field, M. Fisher, Y. Fu, I.K. Furic, J. Gartner, S. Goldberg, J. Hugon, B. Kim, J. Konigsberg, A. Korytov, A. Kropivnitskaya, T. Kypreos, J.F. Low, K. Matchev, G. Mitselmakher, L. Muniz, P. Myeonghun, C. Prescott, R. Remington, A. Rinkevicius, M. Schmitt, B. Scurlock, P. Sellers, N. Skhirtladze, M. Snowball, D. Wang, J. Yelton, M. Zakaria

Florida International University, Miami, USA
V. Gaultney, L.M. Lebolo, S. Linn, P. Markowitz, G. Martinez, J.L. Rodriguez

Florida State University, Tallahassee, USA
T. Adams, A. Askew, J. Bochenek, J. Chen, B. Diamond, S.V. Gleyzer, J. Haas, S. Hagopian, V. Hagopian, M. Jenkins, K.F. Johnson, H. Prosper, S. Sekmen, V. Veeraraghavan

Florida Institute of Technology, Melbourne, USA
M.M. Baarmand, B. Dorney, M. Hohlmann, H. Kalakhety, I. Vodopiyanov

University of Illinois at Chicago (UIC), Chicago, USA
M.R. Adams, I.M. Anghel, L. Apanasevich, Y. Bai, V.E. Bazterra, R.R. Betts, J. Callner, R. Cavanaugh, C. Dragoiu, L. Gauthier, C.E. Gerber, D.J. Hofman, S. Khalatyan, G.J. Kunde[49], F. Lacroix, M. Malek, C. O'Brien, C. Silkworth, C. Silvestre, A. Smoron, D. Strom, N. Varelas

The University of Iowa, Iowa City, USA
U. Akgun, E.A. Albayrak, B. Bilki, W. Clarida, F. Duru, C.K. Lae, E. McCliment, J.-P. Merlo, H. Mermerkaya[50], A. Mestvirishvili, A. Moeller, J. Nachtman, C.R. Newsom, E. Norbeck, J. Olson, Y. Onel, F. Ozok, S. Sen, J. Wetzel, T. Yetkin, K. Yi

Johns Hopkins University, Baltimore, USA
B.A. Barnett, B. Blumenfeld, A. Bonato, C. Eskew, D. Fehling, G. Giurgiu, A.V. Gritsan, Z.J. Guo, G. Hu, P. Maksimovic, S. Rappoccio, M. Swartz, N.V. Tran, A. Whitbeck

The University of Kansas, Lawrence, USA

P. Baringer, A. Bean, G. Benelli, O. Grachov, R.P. Kenny Iii, M. Murray, D. Noonan, S. Sanders, J.S. Wood, V. Zhukova

Kansas State University, Manhattan, USA
A.f. Barfuss, T. Bolton, I. Chakaberia, A. Ivanov, S. Khalil, M. Makouski, Y. Maravin, S. Shrestha, I. Svintradze, Z. Wan

Lawrence Livermore National Laboratory, Livermore, USA
J. Gronberg, D. Lange, D. Wright

University of Maryland, College Park, USA
A. Baden, M. Boutemeur, S.C. Eno, D. Ferencek, J.A. Gomez, N.J. Hadley, R.G. Kellogg, M. Kirn, Y. Lu, A.C. Mignerey, K. Rossato, P. Rumerio, F. Santanastasio, A. Skuja, J. Temple, M.B. Tonjes, S.C. Tonwar, E. Twedt

Massachusetts Institute of Technology, Cambridge, USA
B. Alver, G. Bauer, J. Bendavid, W. Busza, E. Butz, I.A. Cali, M. Chan, V. Dutta, P. Everaerts, G. Gomez Ceballos, M. Goncharov, K.A. Hahn, P. Harris, Y. Kim, M. Klute, Y.-J. Lee, W. Li, C. Loizides, P.D. Luckey, T. Ma, S. Nahn, C. Paus, D. Ralph, C. Roland, G. Roland, M. Rudolph, G.S.F. Stephans, F. Stöckli, K. Sumorok, K. Sung, D. Velicanu, E.A. Wenger, R. Wolf, S. Xie, M. Yang, Y. Yilmaz, A.S. Yoon, M. Zanetti

University of Minnesota, Minneapolis, USA
S.I. Cooper, P. Cushman, B. Dahmes, A. De Benedetti, G. Franzoni, A. Gude, J. Haupt, K. Klapoetke, Y. Kubota, J. Mans, N. Pastika, V. Rekovic, R. Rusack, M. Sasseville, A. Singovsky, N. Tambe, J. Turkewitz

University of Mississippi, University, USA
L.M. Cremaldi, R. Godang, R. Kroeger, L. Perera, R. Rahmat, D.A. Sanders, D. Summers

University of Nebraska-Lincoln, Lincoln, USA
K. Bloom, S. Bose, J. Butt, D.R. Claes, A. Dominguez, M. Eads, P. Jindal, J. Keller, T. Kelly, I. Kravchenko, J. Lazo-Flores, H. Malbouisson, S. Malik, G.R. Snow

State University of New York at Buffalo, Buffalo, USA
U. Baur, A. Godshalk, I. Iashvili, S. Jain, A. Kharchilava, A. Kumar, S.P. Shipkowski, K. Smith

Northeastern University, Boston, USA
G. Alverson, E. Barberis, D. Baumgartel, O. Boeriu, M. Chasco, S. Reucroft, J. Swain, D. Trocino, D. Wood, J. Zhang

Northwestern University, Evanston, USA
A. Anastassov, A. Kubik, N. Mucia, N. Odell, R.A. Ofierzynski, B. Pollack, A. Pozdnyakov, M. Schmitt, S. Stoynev, M. Velasco, S. Won

University of Notre Dame, Notre Dame, USA
L. Antonelli, D. Berry, A. Brinkerhoff, M. Hildreth, C. Jessop, D.J. Karmgard, J. Kolb, T. Kolberg, K. Lannon, W. Luo, S. Lynch, N. Marinelli, D.M. Morse, T. Pearson, R. Ruchti, J. Slaunwhite, N. Valls, M. Wayne, J. Ziegler

The Ohio State University, Columbus, USA
B. Bylsma, L.S. Durkin, J. Gu, C. Hill, P. Killewald, K. Kotov, T.Y. Ling, M. Rodenburg, C. Vuosalo, G. Williams

Princeton University, Princeton, USA
N. Adam, E. Berry, P. Elmer, D. Gerbaudo, V. Halyo, P. Hebda, A. Hunt, E. Laird, D. Lopes

Pegna, D. Marlow, T. Medvedeva, M. Mooney, J. Olsen, P. Piroué, X. Quan, B. Safdi, H. Saka, D. Stickland, C. Tully, J.S. Werner, A. Zuranski

University of Puerto Rico, Mayaguez, USA
J.G. Acosta, X.T. Huang, A. Lopez, H. Mendez, S. Oliveros, J.E. Ramirez Vargas, A. Zatserklyaniy

Purdue University, West Lafayette, USA
E. Alagoz, V.E. Barnes, G. Bolla, L. Borrello, D. Bortoletto, M. De Mattia, A. Everett, A.F. Garfinkel, L. Gutay, Z. Hu, M. Jones, O. Koybasi, M. Kress, A.T. Laasanen, N. Leonardo, C. Liu, V. Maroussov, P. Merkel, D.H. Miller, N. Neumeister, I. Shipsey, D. Silvers, A. Svyatkovskiy, M. Vidal Marono, H.D. Yoo, J. Zablocki, Y. Zheng

Purdue University Calumet, Hammond, USA
S. Guragain, N. Parashar

Rice University, Houston, USA
A. Adair, C. Boulahouache, K.M. Ecklund, F.J.M. Geurts, B.P. Padley, R. Redjimi, J. Roberts, J. Zabel

University of Rochester, Rochester, USA
B. Betchart, A. Bodek, Y.S. Chung, R. Covarelli, P. de Barbaro, R. Demina, Y. Eshaq, H. Flacher, A. Garcia-Bellido, P. Goldenzweig, Y. Gotra, J. Han, A. Harel, D.C. Miner, G. Petrillo, W. Sakumoto, D. Vishnevskiy, M. Zielinski

The Rockefeller University, New York, USA
A. Bhatti, R. Ciesielski, L. Demortier, K. Goulianos, G. Lungu, S. Malik, C. Mesropian

Rutgers, the State University of New Jersey, Piscataway, USA
S. Arora, O. Atramentov, A. Barker, C. Contreras-Campana, E. Contreras-Campana, D. Duggan, Y. Gershtein, R. Gray, E. Halkiadakis, D. Hidas, D. Hits, A. Lath, S. Panwalkar, R. Patel, A. Richards, K. Rose, S. Schnetzer, S. Somalwar, R. Stone, S. Thomas

University of Tennessee, Knoxville, USA
G. Cerizza, M. Hollingsworth, S. Spanier, Z.C. Yang, A. York

Texas A&M University, College Station, USA
R. Eusebi, W. Flanagan, J. Gilmore, A. Gurrola, T. Kamon, V. Khotilovich, R. Montalvo, I. Osipenkov, Y. Pakhotin, A. Perloff, A. Safonov, S. Sengupta, I. Suarez, A. Tatarinov, D. Toback

Texas Tech University, Lubbock, USA
N. Akchurin, C. Bardak, J. Damgov, P.R. Dudero, C. Jeong, K. Kovitanggoon, S.W. Lee, T. Libeiro, P. Mane, Y. Roh, A. Sill, I. Volobouev, R. Wigmans, E. Yazgan

Vanderbilt University, Nashville, USA
E. Appelt, E. Brownson, D. Engh, C. Florez, W. Gabella, M. Issah, W. Johns, C. Johnston, P. Kurt, C. Maguire, A. Melo, P. Sheldon, B. Snook, S. Tuo, J. Velkovska

University of Virginia, Charlottesville, USA
M.W. Arenton, M. Balazs, S. Boutle, B. Cox, B. Francis, S. Goadhouse, J. Goodell, R. Hirosky, A. Ledovskoy, C. Lin, C. Neu, J. Wood, R. Yohay

Wayne State University, Detroit, USA
S. Gollapinni, R. Harr, P.E. Karchin, C. Kottachchi Kankanamge Don, P. Lamichhane, M. Mattson, C. Milstène, A. Sakharov

University of Wisconsin, Madison, USA
M. Anderson, M. Bachtis, D. Belknap, J.N. Bellinger, D. Carlsmith, M. Cepeda, S. Dasu, J. Efron, L. Gray, K.S. Grogg, M. Grothe, R. Hall-Wilton, M. Herndon, A. Hervé, P. Klabbers, J. Klukas, A. Lanaro, C. Lazaridis, J. Leonard, R. Loveless, A. Mohapatra, I. Ojalvo, W. Parker, I. Ross, A. Savin, W.H. Smith, J. Swanson, M. Weinberg

†: Deceased
1: Also at CERN, European Organization for Nuclear Research, Geneva, Switzerland
2: Also at Universidade Federal do ABC, Santo Andre, Brazil
3: Also at California Institute of Technology, Pasadena, USA
4: Also at Laboratoire Leprince-Ringuet, Ecole Polytechnique, IN2P3-CNRS, Palaiseau, France
5: Also at Suez Canal University, Suez, Egypt
6: Also at British University, Cairo, Egypt
7: Also at Fayoum University, El-Fayoum, Egypt
8: Also at Ain Shams University, Cairo, Egypt
9: Also at Soltan Institute for Nuclear Studies, Warsaw, Poland
10: Also at Massachusetts Institute of Technology, Cambridge, USA
11: Also at Université de Haute-Alsace, Mulhouse, France
12: Also at Moscow State University, Moscow, Russia
13: Also at Brandenburg University of Technology, Cottbus, Germany
14: Also at Institute of Nuclear Research ATOMKI, Debrecen, Hungary
15: Also at Eötvös Loránd University, Budapest, Hungary
16: Also at Tata Institute of Fundamental Research - HECR, Mumbai, India
17: Also at University of Visva-Bharati, Santiniketan, India
18: Also at Sharif University of Technology, Tehran, Iran
19: Also at Isfahan University of Technology, Isfahan, Iran
20: Also at Shiraz University, Shiraz, Iran
21: Also at Facoltà Ingegneria Università di Roma, Roma, Italy
22: Also at Università della Basilicata, Potenza, Italy
23: Also at Laboratori Nazionali di Legnaro dell' INFN, Legnaro, Italy
24: Also at Università degli studi di Siena, Siena, Italy
25: Also at Faculty of Physics of University of Belgrade, Belgrade, Serbia
26: Also at University of California, Los Angeles, Los Angeles, USA
27: Also at University of Florida, Gainesville, USA
28: Also at Université de Genève, Geneva, Switzerland
29: Also at Scuola Normale e Sezione dell' INFN, Pisa, Italy
30: Also at INFN Sezione di Roma; Università di Roma "La Sapienza", Roma, Italy
31: Also at University of Athens, Athens, Greece
32: Also at The University of Kansas, Lawrence, USA
33: Also at Paul Scherrer Institut, Villigen, Switzerland
34: Also at University of Belgrade, Faculty of Physics and Vinca Institute of Nuclear Sciences, Belgrade, Serbia
35: Also at Institute for Theoretical and Experimental Physics, Moscow, Russia
36: Also at Gaziosmanpasa University, Tokat, Turkey
37: Also at Adiyaman University, Adiyaman, Turkey
38: Also at The University of Iowa, Iowa City, USA
39: Also at Mersin University, Mersin, Turkey
40: Also at Izmir Institute of Technology, Izmir, Turkey
41: Also at Kafkas University, Kars, Turkey
42: Also at Suleyman Demirel University, Isparta, Turkey

43: Also at Ege University, Izmir, Turkey
44: Also at Rutherford Appleton Laboratory, Didcot, United Kingdom
45: Also at School of Physics and Astronomy, University of Southampton, Southampton, United Kingdom
46: Also at INFN Sezione di Perugia; Università di Perugia, Perugia, Italy
47: Also at Utah Valley University, Orem, USA
48: Also at Institute for Nuclear Research, Moscow, Russia
49: Also at Los Alamos National Laboratory, Los Alamos, USA
50: Also at Erzincan University, Erzincan, Turkey